

National Report of Poland to EUREF 2020/2021

J. Krynski

Institute of Geodesy and Cartography, 27 Modzelewskiego St., 02-679 Warsaw

E-mail: krynski@igik.edu.pl

J.B. Rogowski

Gdynia Maritime University, 81-87 Morska St., 81-225 Gdynia

E-mail: jerzyrogowski@gmail.com

1. Introduction

Since 2018 the main geodetic activities at the national level in Poland concentrated on maintenance horizontal, vertical, gravity and geomagnetic control, continuing operational work of permanent IGS/EPN GNSS stations, GNSS data processing on the regular basis at the WUT and MUT Analysis Centres, activities of MUT and WUT EPN Combination Centre, activity within the EUREF-IP Project, works on GNSS for meteorology, monitoring ionosphere and ionospheric storms, GNSS receiver antenna calibration, advanced methods for satellite positioning, improving consistency between SLR and GNSS solution, GNSS for navigation, maintaining the ASG-EUPOS network in Poland, modelling precise geoid, the use of data from satellite gravity missions, monitoring gravity changes, activities in satellite laser ranging and their use, geodynamics.

2. Current status of reference frames

Research activities of Polish research groups in a period of 2015–2018 on reference frames and reference networks were reviewed and summarised (Krynski et al., 2019a). The results concerning the implementation of latest resolutions on reference systems of the International Union of Geodesy and Geophysics (IUGG) and the International Union of Astronomy (IAU) with special emphasis on the changes in the Astronomical Almanac of the Institute of Geodesy and Cartography, Warsaw were presented. The status of the implementation of ETRS89 in Poland, monitoring the terrestrial reference frame, operational work of GNSS permanent IGS/EPN stations and the laser ranging station of the International Laser Ranging Service (ILRS) in Poland, active GNSS station network for the realization of ETRS89 in Poland, validation of recent ETRS89 realization, expressed in ETRF2000 in Poland, and maintenance of the vertical control in Poland (PL-KRON86-NH) were discussed. Extensive research activities are observed in the field of maintenance and modernization of gravity control not only in Poland, but also in Sweden and in Denmark, as well as establishment of gravity control in Ireland based on absolute gravity survey.

The magnetic control in Poland was also regularly maintained.

After the geodetic and cartographic act amendment, since 31 July 2020 all the data concerning the geodetic (including GNSS observations), gravimetric, and magnetic control networks are available free of charge. The data have been published on the national geoport¹.

2.1. Horizontal and vertical

The Head Office of Geodesy and Cartography (GUGiK) continued a field inspection of geodetic fundamental and base control network points.

2.2. Vertical

In 2020 GUGiK initiated works related to the new levelling campaign in Poland. In cooperation with the State Service of Ukraine for Geodesy, Cartography and Cadastre, two cross-border levelling junctions were conducted (the levelling lines: Chelm-Kovel and Przemysl-Lviv). Levelling surveys were performed on the testing area to develop the methodology for the levelling campaign, in particular to compare the accuracy of GNSS levelling with precise geometric levelling.

The PL-EVRF2007-NH is in the process of implementation by local authorities. According to the Polish regulations, the EVRF2007 solution should be implemented locally by the end of 2023, at latest. The quasigeoid model PL-geoid-2011 for the PL-EVRF2007-NH was published on the GUGiK website².

Recent status of the realization of the International Height Reference System was discussed (Lyszkowicz, 2019) preceded with the review of the activities concerning the establishment of the global height system undertaken by the IAG in the last 30 years including the IAG resolution concerning the definition of the global height system as well as a draft of the global vertical network and possible scenarios for the determination gravity potential at the points of this network. Planned works on the detail realization of the global vertical network in the near future are also described.

¹ <http://www.gugik.gov.pl>

² <http://www.gugik.gov.pl/bip/prawo/modele-danych>

2.3. Gravity

Activities of the Polish research concerning gravity field modelling and gravimetry in a period of 2015–2018 were reviewed and summarised (Krynski et al., 2019b). The results of research on the evaluation of GOCE-based global geopotential models (GGMs) in Poland and geoid modelling. Extensive research activities are observed in the field of absolute gravity surveys, in particular for the maintenance of national gravity control in Poland, Sweden, Denmark, the Republic of Ireland and in Northern Ireland as well as for geodynamics with special emphasis on metrological aspects in absolute gravimetry were presented. Long term gravity variations were monitored in two gravimetric laboratories: the Borowa Gora Geodetic-Geophysical Observatory, and Jozefoslaw Astrogeodetic Observatory with the use of quasi-regular absolute gravity measurements as well as tidal gravimeter records. Gravity series obtained were analysed considering both local and global hydrology effects. Temporal variations of the gravity field were investigated using data from GRACE satellite mission as well as SLR data. Estimated variations of physical heights indicate the need for kinematic realization of reference surface for heights. Also seasonal variability of the atmospheric and water budgets in Poland was a subject of investigation in terms of total water storage using the GLDAS data. The use of repeatable absolute gravity data for calibration/validation of temporal mass variations derived from satellite gravity missions was discussed. Also contribution of gravimetric records to seismic studies was investigated.

Research activities concerning gravimetric reference frames in Poland or performed by Polish institutions abroad in 2019 and 2020 focused around regular absolute gravity surveys with two Polish absolute gravimeters FG5-230 (Warsaw University of Technology – WUT) and A10-020 (Institute of Geodesy and Cartography – IGIK) at their respective Observatories as well as analysis of records of the superconducting gravimeter at the Borowa Gora Geodetic-Geophysical Observatory (BG) of IGIK, metrological aspects in gravimetry and investigations of the non-tidal gravity changes.

Maintenance of gravity reference value in Poland

In 2019 the long period quasi-monthly monitoring of the absolute gravity at the Jozefoslaw Astrogeodetic Observatory (JO) of WUT was continued using the FG5-230 ballistic gravimeter. Since 2005 when the observations has been started almost 15 years long time series was acquired (Krynski et al., 2019b) (Fig. 1). Ground water level was recorded by hydrostatic piezometer and five soil moisture sensors from 0.5 m to 6.0 m depth

(Krynski and Rogowski, 2019). Repeated absolute gravity measurements with the FG5-230 gravimeter as well as tidal observations with the LCR ET gravimeter have been terminated in January 2020 due to major renovation of the Jozefoslaw Observatory. The measurements with IGRF requirements standards are planned to start in July 2021. During this break absolute gravity measurements are conducted with the FG5-230 twice a year on the stations of the Polish Geological Institute; the LCR ET gravimeter has been moved to BG where it continuously operates with LCR G spring gravimeters as well as with the SG iGrav-027.

Gravimetric investigations at BG were continued with two breaks, first at the beginning of 2019 and then in mid-2020, resulting from the A10-020 regular maintenance and service at Micro-g LaCoste Inc. in both years as well as limited survey possibilities due to Covid-19 pandemic. A series of absolute gravity measurements on three stations of the test network in the Observatory, conducted on monthly basis with the A10-020 gravimeter since September 2008 (Fig. 2), shows high quality of A10 gravimeter results.

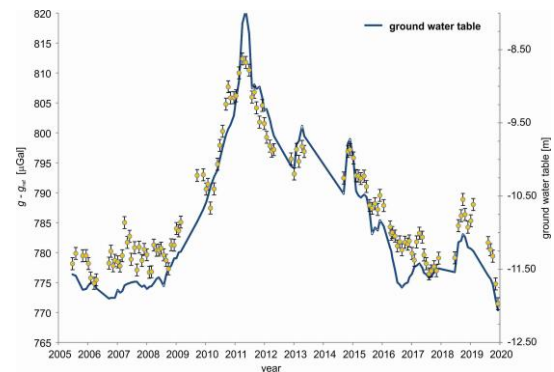


Fig. 1. Absolute gravity surveyed with the FG5-230 at Jozefoslaw (100 cm height) ($g_{ref} = 981213000 \mu\text{Gal}$)

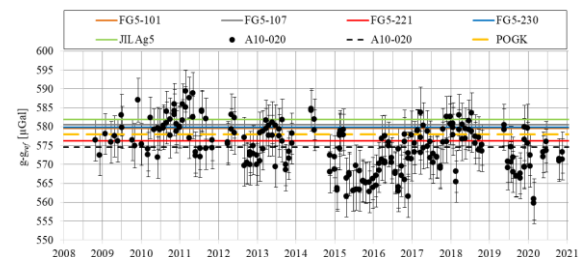


Fig. 2. Absolute gravity surveyed with the A10-020 at A-BG station in Borowa Gora (pillar level) ($g_{ref} = 981250000 \mu\text{Gal}$)

Since 2016 the iGrav-027 superconducting gravimeter is co-located with BG-G2 station of the test network of BG Observatory. In 2019 an AG/SG analysis was performed with the use of A10-020 and iGrav-027 gravimeter in order to monitor gravity reference function at Borowa Gora Observatory (Dykowski et. al., 2019c). The record

of nearly 1080 days of the iGrav gravimeter was analysed. The drift of the iGrav-027 was evaluated using surveys with the A10-020 gravimeter. Drift corrected residual of the iGrav-027 gravimeter together with A10-020 monthly gravity values on the BG-G2 station updated for 2019 and 2020 results is presented in Figure 3. Additionally results in Figure 3 were referred to the mean gravity reference level from the final results of the EURAMET absolute gravimeter comparison in Wettzell in 2018 (Falk et al., 2020). Within more than four years analysed, peak to peak gravity variation exceeding 200 nm/s² of the gravity reference function is observed. Combined AG/SG results allowed to evaluate the consistency of the A10-020 absolute gravimeter at 36.7 nm/s² with respect to the iGrav-027. These analyses are planned to be continued allowing Borowa Gora Observatory to meet the requirements for an IGRS reference station.

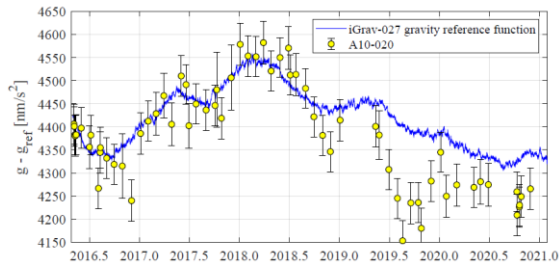


Fig. 3. Gravity determined with the A10-020 and iGrav-027 gravimeters from more than four years of operation at the Borowa Gora Observatory ($g_{ref} = 981250000 \mu\text{Gal}$)

Also an annual comparison of absolute gravimeters FG5-230 and A10-020 was carried out in October 2019 at the Geodetic-Geophysical Observatory in Borowa Gora. Due to Covid-19 no such comparison was performed in 2020.

Both Observatories Borowa Gora and Jozefoslaw are considered as future reference stations in the currently developed International Gravity Reference Frame (IGRF) as they perform absolute gravity surveys on regular basis. Additionally Borowa Gora supplements AG surveys with gravity time series from the superconducting gravimeter iGrav-027.

Maintenance of gravity controls in Europe

The results of absolute gravity survey in Sweden with the A10-020 gravimeter in 2011–2015 were used in the definition of the new gravity reference frame of Sweden – RG 2000 (Engfeldt et al., 2019).

The A10-020 gravimeter was further used in 2019 for the establishment of the gravity control on Ireland island (Dykowski et al., 2019a, 2019c). In 2019 both gravity and the vertical gravity gradient were partially determined at 41 of 64 gravity control stations. Together in 2018 and 2019 gravity surveys were completed on all 6 calibration baseline

stations, all 7 IGSN71 stations. Vertical gravity gradients were determined on all 51 network stations and absolute gravity surveys with the A10-020 were completed on 37 out of 51 stations (Fig. 4). Due to Covid-19 pandemic further works in Ireland were not continued in 2020.

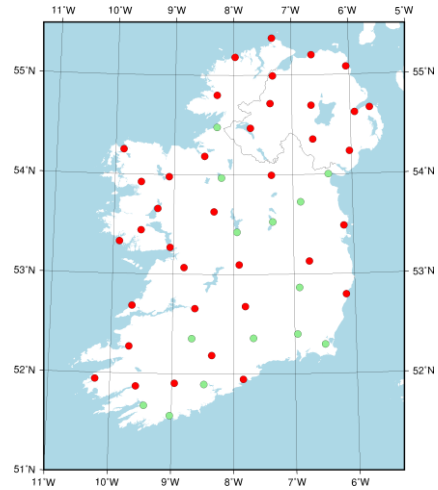


Fig. 4. Gravity control in Ireland – network stations: red – both absolute and vertical gravity gradient surveys done, green – vertical gravity gradient survey done only

The fifth local calibration meeting of absolute gravimeters FG5-230 and A10-020 (properties of the Institute of Geodesy and Cartography) was carried out in 2019 at the Geodetic-Geophysical Observatory Borowa Gora.

2.4. Magnetic

Magnetic control in Poland, consisting of 19 magnetic repeat stations maintained by IGIK is supported by two magnetic observatories run by the Institute of Geophysics of the Polish Academy of Sciences (IGF PAS): Central Geophysical Observatory in Belsk and Magnetic Observatory in Hel. In addition, there are two permanent magnetic stations: Borowa Gora – run by IGIK, and Suwalki – run by IGF PAS (Fig. 5).

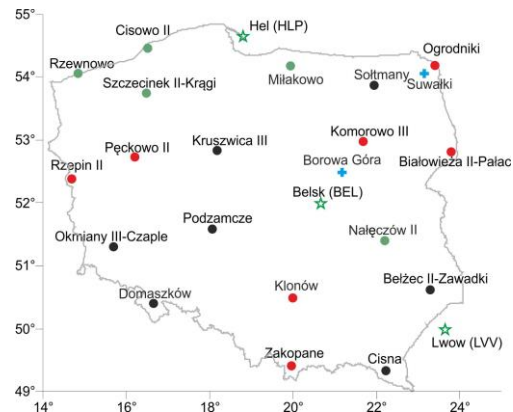


Fig. 5. Magnetic stations surveyed in 2019 (red dots), in 2020 (green dots), and magnetic observatories

Measurements of three independent components of the magnetic intensity vector, i.e. declination (D), inclination (I) and the module of the magnetic intensity vector (F) were performed in 2019 and in 2020 at 7 and 5 repeat stations of the fundamental magnetic control, respectively (Fig. 5).

3. Participation in IGS/EPN permanent GNSS networks

3.1. Operational work of permanent IGS/EPN stations

Permanent IGS and EPN GNSS stations operate in Poland since 1993. Recently 19 permanent GNSS stations (Table 1) operate in Poland within the EUREF program of which 6 operate also within the IGS network³ (Fig. 6). Data from those stations are transferred via internet to two Regional Data Centres, located at BEV in Vienna, Austria, and BKG in Frankfurt/Main, Germany. Together with data from other corresponding stations in Europe, they were the basis of the products that are applied for both research and practical use in geodesy, surveying, precise navigation, environmental projects, etc.

Four of those stations, i.e. BOGI, BOR1, JOZ2 and WROC participated also in IGS Real-time GNSS Data project. Two stations WROC and BOR1 are also included into the IGS Multi-GNSS Experiment (MGEX) pilot project⁴.



Fig. 6. EPN/IGS permanent GNSS stations in Poland (2020)

The EPN stations at Borowa Gora (BOGI) (temporary unavailable), Borowiec (BOR1) (temporary unavailable), Jozefoslaw (JOZ2, JOZ3), Cracow (KRAW, KRA1), Lamkowko (LAM5), and Wroclaw (WROC) take part in the EUREF-IP project⁵ (Fig. 7).

Since March 2005 Ntrip Broadcaster is installed at the AGH University of Science and Technology⁶. The Ntrip Caster broadcasts RTCM and raw GNSS data from KRAW0 and KRA10 sources take part in the EUREF-IP project and provide data to regional EUREF broadcasters at BKG, ASI and ROB.



Fig. 7. Polish EPN stations participating in the EUREF-IP project (2020)

Table 1. Permanent GNSS stations in Poland (2020)

Name (abbreviation)	Latitude	Longitude	Status
Biala Podlaska (BPD)	52°02'07"	23°07'38"	EPN
Borowa Gora (BOGE)	52°28'31"	21°02'06"	EPN
Borowa Gora (BOGI)	52°28'30"	21°02'07"	IGS/EPN
Borowa Gora (BOGO)	52°28'33"	21°02'07"	EPN
Borowiec (BOR1)	52°16'37"	17°04'24"	IGS/EPN
Bydgoszcz (BYDG)	53°08'04"	17°59'37"	EPN
Gorzow Wielk. (GWWL)	52°44'17"	15°12'19"	EPN
Jozefoslaw (JOZE)	52°05'50"	21°01'54"	IGS/EPN
Jozefoslaw (JOZ2)	52°05'52"	21°01'56"	IGS/EPN
Katowice (KATO)	50°15'11"	19°02'08"	EPN
Krakow (KRAW)	50°03'58"	19°55'14"	EPN
Krakow (KRA1)	50°03'58"	19°55'14"	EPN
Lamkowko (LAMA)	53°53'33"	20°40'12"	IGS/EPN
Lodz (LODZ)	51°46'43"	19°27'34"	EPN
Redzikowo (REDZ)	54°28'21"	17°07'03"	EPN
Suwalki (SWKI)	54°05'55"	22°55'42"	EPN
Ustrzyki Dolne (USDL)	49°25'58"	22°35'09"	EPN
Wroclaw (WROC)	51°06'47"	17°03'43"	IGS/EPN
Zywiec (ZYWI)	49°41'12"	19°12'21"	EPN

³ http://www.epncb.oma.be/_networkdata/stationlist.php

⁴ <http://igs.org/mgex>

⁵ http://igs.bkg.bund.de/root_ftp/NTRIP/streams/streamlist_euref-ip.htm

⁶ <http://home.agh.edu.pl/~kraw/ntrip.php>

3.2. GNSS data processing at WUT AC

The WUT EPN Analysis Centre (AC) is operated since 1996. WUT AC contributes to EUREF with final (weekly and daily) and rapid daily solutions of the EPN subnetwork. At the end of 2020, the WUT AC subnetwork (Fig. 8) consisted of 138 GNSS stations (14 new stations were added in 2019 and 2020) from which 97% observed both GPS and GLONASS satellites and 75% observed also Galileo satellites.



Fig. 8. EPN stations providing data processed at WUT EUREF AC (02 April 2021)⁷

GNSS data are processed in WUT AC using the Bernese GNSS Software v.5.2. Since 2010, WUT operational solutions were based on GPS and GLONASS observations. Since GPS week 2044 (10 March 2019), WUT includes also Galileo observations in its operational solutions. Since the week 2075 WUT started using CODE rapid products (GNSS satellite orbits and clock corrections) for the generation of the final products.

In 2018, WUT AC started creating new solutions, in which the WUT regional subnetwork was augmented by global IGS reference stations. The purpose of creating those solutions is to analyze the impact of adding global stations on station coordinates of the regional network. In 2019 and 2020, these activities were continued.

WUT products, i.e., daily and weekly coordinates in SINEX format and zenith tropospheric delays, can be accessed from EPN data centres: BKG⁸ and EPN⁹.

The recent activities of the WUT EPN AC were presented at the EUREF Analysis Centres Workshop held on 16–17 October 2019 in Warsaw (Liwosz, 2019). On 17 May 2020 WUT AC started to use the IGB14 reference frame.

3.3. GNSS data processing at MUT AC

The Military University of Technology in Warsaw (MUT) Analysis Centre (AC) provides final (daily and weekly) and rapid solutions. At the end of 2020 MUT LAC processed data from 153 EPN stations (Fig. 9) distributed homogeneously over Europe. Since GPS week 2081 two new EPN stations from Germany (FFMJ00DEU, TIT200DEU) were added to MUT subnetwork.

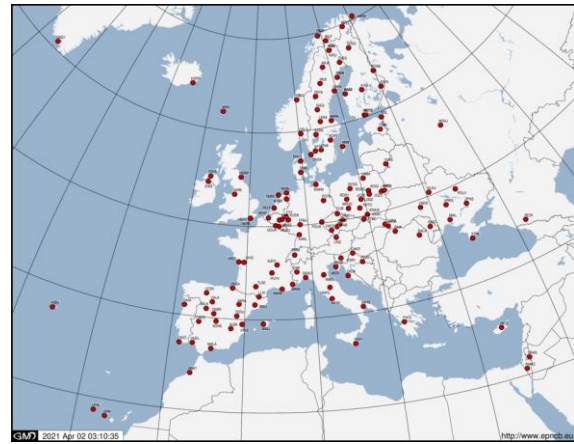


Fig. 9. EPN stations providing data processed at MUT EUREF AC (02 April 2021)¹⁰

Since GPS week 2044 the GNSS (GPS + Galileo) processing is done at MUT AC using GNSS analysis software GAMIT, version 10.70. The change in strategy came after previously conducted tests. Two sets of daily products were prepared, one based on GPS data and the second on Galileo data. Analysis showed that today ambiguity resolutions for GPS and Galileo are at the same level. Also the differences in the coordinate repeatability are pretty small (Fig. 10). There is still a well-known problem with the antenna modelling for the Galileo signal. The use of G02 corrections instead of E05 causes significant differences up to 5 mm in the Up component. However, this problem is expected to be solved with a new IGS release.

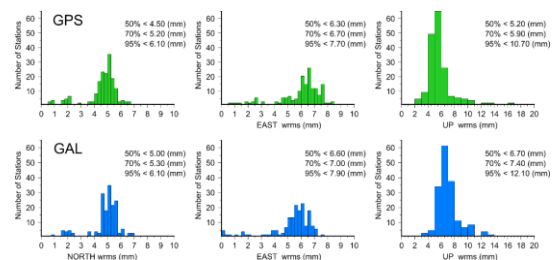


Fig. 10. Coordinate repeatability of GPS-only and Galileo-only solutions

⁷ <http://www.epncb.oma.be/>

⁸ <ftp://igs.bkg.bund.de/EUREF/products>

⁹ <ftp://epncb.oma.be/epncb/product/clusters>

¹⁰ <http://www.epncb.oma.be/>

MUT processes also local GNSS data and provides the station monitoring service¹¹. The processing strategy applied is similar to the one used by the MUT AC for EPN and fully fulfils the EPN Guidelines. In addition to coordinate monitoring also the data QC service is provided. It is based on the G-Nut/Anubis software (Vaclavovic and Dousa, 2016).

The GNSS Data Research Infrastructure Centre (CIBDG) which creates the GNSS data repository in Poland, is under construction at MUT AC in the framework of the project of the European Regional Development Fund co-financed by EU. CIBDG will become the national node for the EPOS (European Plate Observing System) project. The repository archives observation data from all GNSS stations located in the country and belonging to domestic institutions.

Homogenization of solutions for all GNSS stations in Poland is carried out in the framework of the EPOS project. It is crucial from the point of view of the stability of the reference system in the country and the possibility of using GNSS data to study the age-old deformations of the territory of Poland. The new coordinate monitoring service RefMON (Fig. 11) launched in 2019 presents the quality of observations, current coordinates of the stations, their deviations from those published in the RT services and tropospheric delay over Poland (previous day).

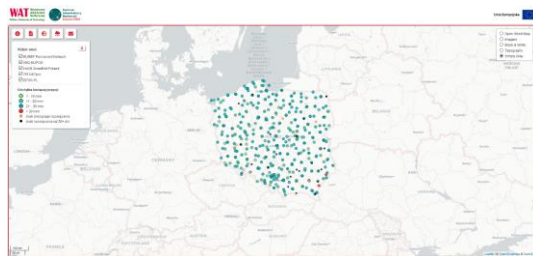


Fig. 11. Webpage of the coordinate monitoring service RefMON that is one of the services of CIBDG¹²

The infrastructure of the MUT AC is also used to analyse land deformation in areas with mining operations (Mutke et al., 2019) in order to assess the impact of humans on the environment. Mobile GNSS sets based on low-cost multi-GNSS cards continuously record position changes of selected points over active coal mines (Fig. 12).

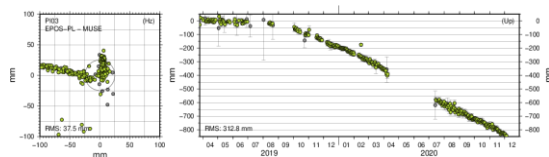


Fig. 12. Displacement of the point located in the mining area

3.4. Activities of MUT and WUT EPN Combination Centre

In 2019 and 2020, the EPN Analysis Combination Centre (ACC) continued to combine GNSS coordinate solutions, provided in the SINEX format, by 16 EPN Analysis Centres into official EPN solutions.

In 2019, a test phase concerning the evaluation of the impact of adding Galileo observations on combined EPN station positions was finished. The comparison between the two-system (GPS, GLONASS) operational coordinate solutions and the three-system (GPS, GLONASS, Galileo) test solutions showed that for the majority of stations mean position differences (over 44 weeks of daily solutions) were below 1 mm in horizontal components and 3 mm in the vertical component (Fig. 13). It was also noted that larger differences were obtained for stations with type mean calibrated antennas than for stations with individually calibrated antennas, especially for the vertical component (Liwosz et al., 2019). Since 10 March 2019 (GPS week 2044), 11 ACs have started officially including Galileo observations in operational products (Liwosz and Araszkiewicz, 2019a).

The impact of adding global stations to the EPN regional network on EPN station positions was also analysed by the EPN ACC in 2019. Good position agreement between the combined solution with global stations and the operational EPN solution (regional) was obtained, and the differences between them mostly came from the alignment of both solutions to the terrestrial reference frame. These differences in the reference frame alignment are caused mainly by the non-tidal loading effects (due to atmosphere and continental water).

The recent activities of the EPN ACC were presented at the EUREF Analysis Centres Workshop held in 16–17 October 2019 in Warsaw (Liwosz and Araszkiewicz, 2019b)

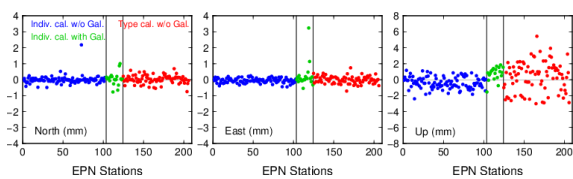


Fig. 13. Mean differences of station positions between combined three-system (GPS, GLONASS, and Galileo) test solutions and EPN combined two-system (GPS and GLONASS) operational solutions

Since the week 2106 (17 May 2020) the daily and weekly combined solutions have been aligned to the new IGS reference frame, i.e. IGB14, which is an updated version of the previously used IGS14. The IGB14 reference frame contains 15 more EPN reference stations (49 stations in total) that can be

¹¹ http://www.gnss.wat.edu.pl/cibdg/refmon/mutr_new.html

¹² <http://www.gnss.wat.edu.pl/gnsswat/>, in Polish

used for the alignment of combined solutions. After the switch, a slightly better agreement of EPN combined solutions with the IGS reference frame was observed, especially for the vertical component. Also, in 2020 the ASI AC (Centro di Geodesia Spaziale G. Colombo, Italy) prepared test solutions using a new software – GipsyX, based on GPS, GLONASS, and Galileo observations. The new solutions have been tested by ACC and showed good agreement with the combined solution. In January 2021, the solutions computed using GipsyX became the operational ASI solutions, and replaced the GPS-only solutions computed with the older GIPSY-OASIS software.

3.5. Other EPN and IGS activities

GNSS for meteorology

The cooperation of the University of Warmia and Mazury in Olsztyn (UWM) with the Shanghai Astronomical Observatory (SHAO) of the Chinese Academy of Sciences (CAS) and Federal University of Pará, Brazil, resulted in research on the assessment of GNSS Integrated Water Vapor (IWV) estimates over central and north-eastern Amazonia, Brazil (Mota et al., 2019). In the study the spatiotemporal distribution of GNSS IWV, IWV products from Moderate Resolution Imaging Spectroradiometer (MODIS) and radiosonde, jointly with surface meteorological data in the state of Rio de Janeiro were analysed (Fig. 14). The results of the study demonstrate the importance of the GNSS in meteorology and climate applications, especially in regions with low density of conventional/automatic stations and/or meteorological radars, like in Amazonia. This work recommends the magnification of the GNSS network in the state of Rio de Janeiro with the meteorological stations collocated near every GNSS receiver, aiming to improve local IWV estimates and serving as additional support for operational numerical assimilation, weather forecast, and nowcast of extreme rainfall and flooding events.

Other research conducted at UWM concerned the analysis of the impact of different GNSS antenna calibrations models on the quality of the tropospheric estimate series for climate applications (Krzan and Stepniak, 2019a, 2019b). Two years of GNSS data collected at 19 European Reference Frame (EUREF) Permanent GNSS Network (EPN) stations were processed with NAPEOS software using the PPP technique. Three different antenna models were used: International GNSS Service (IGS) type-mean Phase Center Correction (PCC) models; PCC models from individual field robot calibration, and calibration in anechoic chamber. All three solutions were processed several times – using GPS only, Galileo only, GPS+GLONASS, GPS+Galileo and multi-GNSS

(GPS+GLONASS+Galileo) observations. In order to validate and assess the quality of the GNSS solutions, tropospheric parameters obtained from ERA-Interim reanalysis were compared with GNSS estimates (Fig. 15).

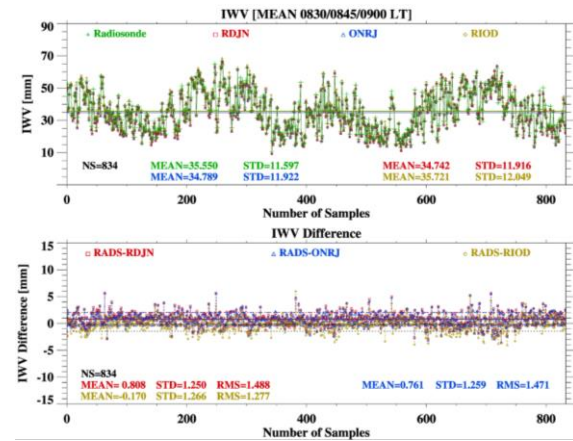


Fig. 14. Time series and statistics (NS, mean, STD, and RMS) of Radiosonde- and GNSS-IWV and the differences from Radiosonde

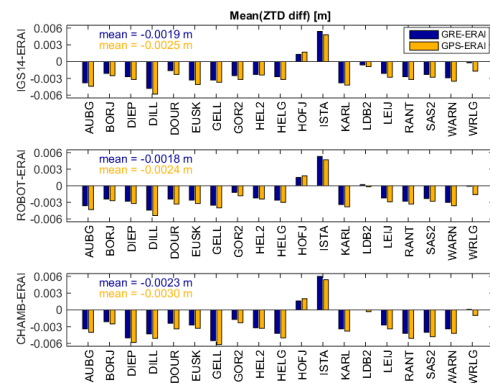


Fig. 15. Mean ZTD differences between [GPS+GLO+GAL] processing (PPP) and ERA-Interim (navy blue) as well as GPS only processing (zero-differenced network solution) and ERA-Interim (orange), 2017

The Institute of Geodesy and Geoinformatics at the Wrocław University of Environmental and Life Sciences (WUELS) maintains the analysis centre for near real-time (NRT) troposphere state retrieval for meteorology purpose. The analysis centre is a part of E-GVAP¹³ since 2012 and is delivering zenith troposphere total delay (ZTD) for GNSS stations belonging to ASG-EUPOS, Leica SmartNet and Nadowski Net networks in Poland (Fig. 16). Hourly solutions are referenced to EPN stations using the minimum constrain condition.

The results from the new ultra-fast NRT (NRT UF) processing of GPS data to obtain troposphere parameters and coordinates with a 15-minute estimation interval and minimum latency were

¹³ <http://egvap.dmi.dk/>

demonstrated. The main goal was to find an optimal estimation strategy for troposphere state parameters with a maximum of 15 minutes latency. The NRT ultra-fast processing was tested on a GNSS network in Poland consisting of 28 stations, of which 19 are EUREF Permanent Network (EPN) stations and 9 are part of the ASG-EUPOS network¹⁴ (Fig. 17).

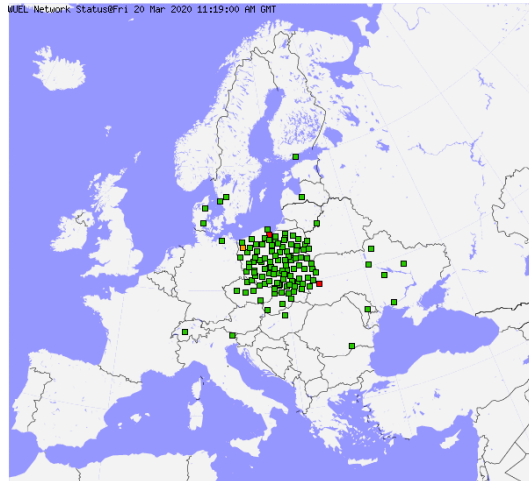


Fig. 16. Map of GNSS stations processed in NRT mode for E-GVAP (status for 2020-03-20)

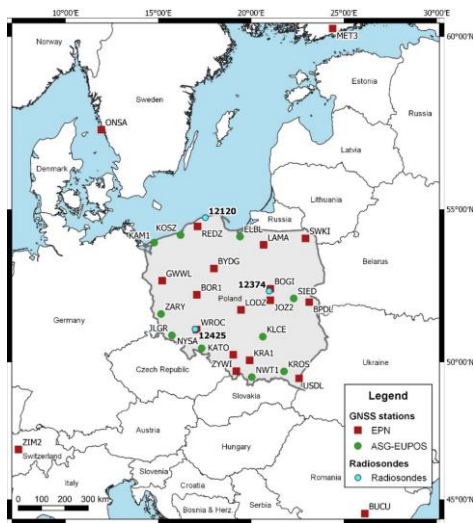


Fig. 17. Map of NRT UF test selected stations

The estimated NRT UF troposphere delays were tested, against 2 different data sets: 1) EPN AC products in common epochs for EPN stations (hourly solution), 2) Final Post-Processing (FPP) solution for all stations considered in this study (15-minute solution) (Fig. 18).

Figure 18 shows that the statistics are consistent for all stations except LAMA, showing small negative biases for the EPN-NRT UF and FPP-NRT UF comparisons. These biases increase with the change from Strategy I to Strategy II. It is worth

noting that the FPP solution is almost identical to the EPN solution for all EPN stations (cyan dots in Fig. 18). The retrieval quality within the time period over which our NRT UF system was tested. It is similar to that of a standard NRT system (5 mm of SDEV). The obtained results proved that tropospheric delay generated by new NRT UF service fulfil the external accuracy criteria.

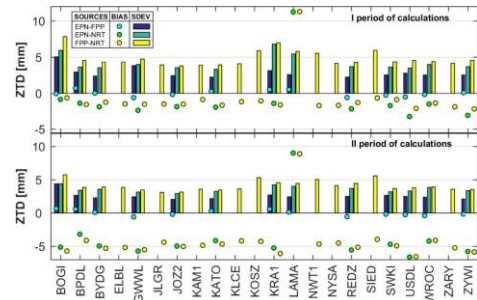


Fig. 18. Statistics of ZTD comparison between EPN AC, FPP, and NRT

The Gdansk University of Technology (GUT) was continuing research related to the use of GNSS tropospheric products on meteorology application (Nykiel et al., 2019a). A derecho occurred in Poland on 11 August 2017 was analysed as a case study. Investigation of this severe weather phenomenon was primarily based on observations from 278 GNSS permanent stations, while data from weather radar and microwave radiometer served for its validation. Zenith tropospheric delay (ZTD) was estimated from the 30-second GNSS observations using Bernese GNSS Software v.5.2 and precise point positioning (PPP) mode. They were converted to the PWV values based on the meteorological data acquired by the synoptic stations. The analysis showed very high convergence between PWV over Poland estimated between 19:30 and 20:30 UTC and refractivity provided by EIG EUMET (Fig. 19).

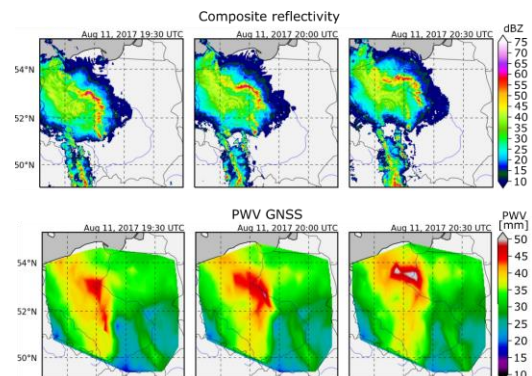


Fig. 19. Composite reflectivity data maps with 2 km spatial resolution (top) and GNSS PWV maps interpolated from observations from the dense network of the GNSS receivers (bottom) over the study area on 11 August 2017 (19:30 to 20:30 UTC) in 30-minute steps

¹⁴ <http://www.asgeupos.pl/>

In addition, dense network of GNSS receivers allowed to show the movement of precipitation zone (identified for PWV exceeding 40 mm) over all analysed area, between 16:30 UTC and 22:00 UTC.

Additional analysis of GNSS gradients has shown even greater usefulness of a dense network of GNSS stations (here one station per 1120 km²) for meteorology application. Both size and direction of gradients estimated at 19:30 UTC and 20:00 UTC clearly pointed storm front (Fig. 20). This clearly confirmed that atmosphere anisotropy indicated by tropospheric gradients reflects changes in the troposphere caused by the weather events.

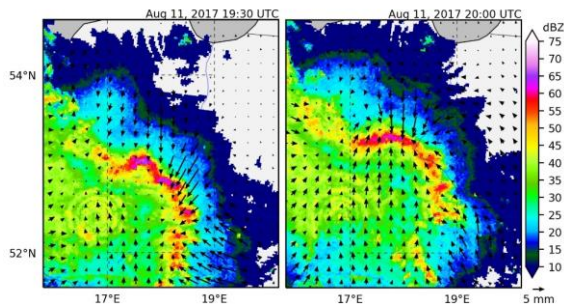


Fig. 20. Gridded gradients estimated from the GNSS observations (left: 19:30 UTC; right: 20:00 UTC) on the background of the composite reflectivity derived from the meteorological radars

GUT undertook activities related to the establishing of a new model for water vapour weighted mean temperature T_m estimation based on the surface temperature T_s (Baldysz et al., 2019). For this purpose radiosonde profiles from 109 evenly distributed in Europe stations, were analysed. Both linear, and non-linear relationship between T_m and T_s were considered, including its dependency from the time of the day. Four models:

- ETm model, obtained by fitting linear regression to the all available data;
- ETm2 model, obtained by fitting linear regression independently for 00:00 UTC and 12: 00 UTC data;
- ETm4 model, obtained by fitting linear regression independently for 00:00 UTC, 06:00 UTC, 12:00 UTC and 18:00 UTC data;
- ETmPoly, obtained by fitting 5th degree polynomial function to the data;

were developed. The ETmPoly model was characterized by the highest accuracy. The T_m estimated using this model and T_m acquired directly from the radiosonde measurement differed the least (RMSE 2.8 ± 0.3 K). These results were more reliable, then those obtained using the Bevis model (RMSE 3.1 ± 0.4 K for the same stations) (Fig. 21).

Additional analysis has also shown the impact of the ETmPoly model on the estimated GNSS PWV values, despite the time of the year. In DJF season

(December, January, February) standard deviations of the discrepancies between PWV estimated using these two models were in the range of 0.02 mm – 0.08 mm, while during JJA (June, July, August) season they were in the range of 0.08 mm – 0.22 mm. The higher differences in JJA resulted from the higher humidity fluctuations in the troposphere, which are better represented by ETmPoly model through taking into account all available synoptic terms.

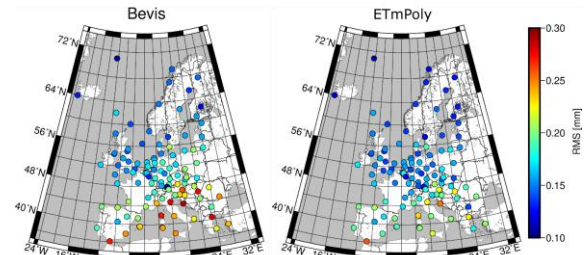


Fig. 21. RMS values of the precipitable water vapour (PWV) estimated using Bevis (left) and ETmPoly (right) coefficients; the PWV derived from RS profiles were adopted as reference

Monitoring ionosphere and ionospheric storms

In 2019, the Institute of Geodesy of UWM continued the studies on the monitoring of ionosphere and ionospheric storms. Several global ionosphere models have been validated in a separate study for different solar activity levels (Wielgosz et al., 2019). The study reveals the advantages and drawbacks of global ionosphere models during severe solar conditions. The monitoring of ionosphere is in parallel focused on the application of different stochastic interpolation techniques together with spherical harmonics (short-wavelength component and long-wavelength component) in the development of regional (in the preliminary research) and consequently – global ionosphere model. The advantages and drawbacks of different techniques are assessed together and tested with independent data from dual frequency altimetry. The application of different stochastic parametric modelling methods to the interpolation of TEC data has been studied with a temporary focus on regional ionosphere models. The enhancement and densification of the global ionosphere models is also considered, and the work on a new global ionosphere model is ongoing. The theoretical background related with the parametrization of Least-Squares Collocation (LSC) is still under studying (Jarmolowski, 2019). However, along with LSC parametrization, the other techniques from the kriging family are studied in parallel to LSC, i.e. Ordinary Kriging (OKR) and Universal Kriging (UKR) (Jarmolowski et al. 2019b). The studies prove similar accuracy of interpolation derived from different parametric

modelling techniques (Fig. 22). However, a special attention should be put on the parametrization and detrending problems related with kriging and LSC.

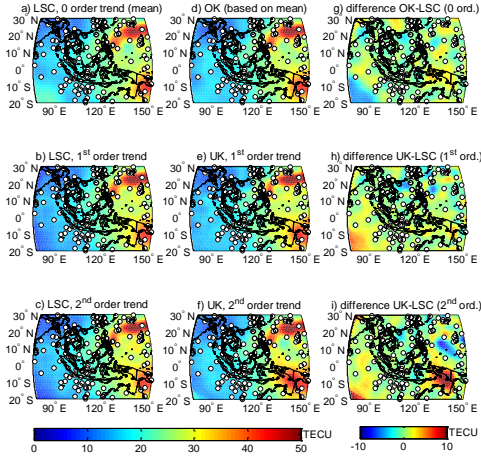


Fig. 22. Regional VTEC models by LSC and kriging, and their differences (4 Feb. 2017, 2:30 UTC)

The application of TEC derived from dual-frequency altimetry missions (Jason-1, Jason-2, Jason-3, Sentinel 3A and 3B) has been studied in the validation of regional ionospheric TEC maps based on GNSS data (Jarmolowski et al., 2019a), as well as the use of ionosonde observations (Krypiak-Gregorczyk et al., 2019). Local model based on Precise Point Positioning and Least Squares Collocation (PPPLSC) as well as global GNSS-based TEC models were validated along the footprints of altimetry orbits. Dual-frequency altimeters provide directly quasi-unbiased TEC signal, and this external validation helps to prove the advantage of stochastic methods in the application to GNSS-based TEC data, which are still sparse in many regions (Jarmolowski et al., 2019) (Fig. 23). This advantage of stochastic techniques is noticeable especially in comparison with the widely used spherical harmonic modelling of the global TEC. Additionally, the impact of different ionosphere models (mainly global due to the global character of LEO observations) have been tested in the units of ionospheric corrections for altimetry ranging. The studies are referred to the coastal regions, which are the zones of merging of altimetry-derived TEC and GNSS-derived TEC. The connection of the datasets in these regions is required, as the dual-frequency altimeters normally determining TEC signal over the oceans cannot measure it over the land, and reversely, GNSS stations dense on the continents are sparse in the ocean zone. Different corrections determined for the altimetric ranges from the variety of global models can differ up to a few centimetres and therefore new, more accurate TEC models are important for altimetry and other LEO satellite missions (Jarmolowski et al., 2018).

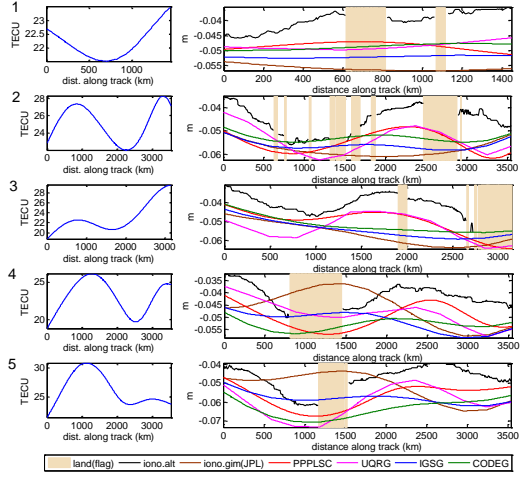


Fig. 23. TEC values interpolated along Jason-3 track from PPPLSC model (left panel); ionospheric corrections for Ku-band along selected tracks from: filtered dual-frequency altimetry, PPPLSC, UQRG, IGSG and CODEG TEC models (right panel). Light brown bars show land derived from surface flags in L2 altimetry product

The studies performed at UWM involved also GNSS-based monitoring the ionosphere at auroral and polar latitudes (Sieradzki and Paziewski, 2018, 2019). The main goal of those investigations was the extension of current methods of ionosphere sounding with an algorithm aimed at extraction of information on large-scale plasma structures. As it is well recognized these irregularities cannot be described with fluctuation or scintillation indices (ROTI, δphi) due to the short time spans used for their computation. Moreover, in such case VTEC maps have also a few limitations such as too low temporal resolution or lack of geometrical dependency required for STEC to VTEC conversion. Thus, in order to detect large-scale ionospheric structures, the authors proposed to use the relative STEC values derived directly from geometry-free combination of phase data (L_4). Although the idea to take the benefit of such indicator is basically not new, the proposed methodology allows the combined processing of network-derived GNSS data. The algorithm consists of two main steps: repairing cycle slips in time series of phase measurements and assessment of background STEC variations. As shown in the indicated above works, the first of them can be realized with a modified approach given by Liu (2011) or a use of moving average of combination P_4. The application of less precise code data in the latter case elevates the noise but is more stable for extreme STEC variations. The second step of algorithm is aimed at an approximation of STEC variations not related to ionospheric disturbances, which involve long-term daily pattern of the electron content as well as a change of elevation angle. This background STEC variations are

computed separately for each clean arc of phase data and, as shown our tests, can be defined with 4-degree polynomial. Taking into account the dynamics of high latitude ionosphere, the applied process of fitting depends on scale of variations observed in geometry-free data. In specific, for quiet conditions the polynomial fitted to all data was adopted, whereas for disturbed ionosphere the process was realized iteratively removing points with extreme values. Finally, the relative STEC values were computed as difference between time series of L_4 and the fitted function. The main advantage of such indicator is providing the information on enhancement of STEC for each epoch, what in turn allows the detailed investigations of ionospheric conditions in time domain.

The analysis of the applicability of the relative STEC values given in Sieradzki and Paziewski (2019) proved that the new indicator allows the detection of large-scale ionospheric structures occurring at high latitudes. In specific, the generated examples of multi-station solution revealed the clear signatures of polar patches, storm enhanced density (SED) and ionospheric trough. Furthermore, the comparison of results performed with the relative STEC values and commonly used ROTI indicate on much higher efficiency of the former solution. This confirms that the applied indicator should be considered as an interesting alternative for other methods of ionosphere sounding. The more detailed investigations on polar patches depicted the strong dependence of these structures on interplanetary magnetic field (IMF) conditions, what is consistent with the knowledge on their origin. Moreover, validation of the relative STEC values with SWARM data confirmed the agreement between both techniques. These combined results suggest that the common application of both dataset should bring the more comprehensive view of high latitude ionosphere.

Sieradzki and Paziewski (2018) investigated also a capability of continuous detection of polar patches with the relative STEC values. The ionospheric conditions on both hemispheres were analysed, and thus, the additional goal was the comparison of these structures. The study proved that larger number of stations on the northern hemisphere implicate more favourable conditions for permanent detection of patches. The situation near the South pole is noticeably worse, but it also allows the identification of structures traveling across the polar cap. The investigations confirmed the simultaneous occurrence of polar patches on both hemispheres. On the other hand, they strongly varied in size and these observed near the South pole were much more massive. The reason of this disproportion seems to be a very dense stream of mid-latitudes plasma, which was detected on the southern hemisphere.

The team of the GUT have continued research related to the analysis of ionospheric disturbances based on GNSS observations. The method of estimating the height of the ionospheric inhomogeneities (HII) based on the network of GNSS receivers was developed (Nykiel et al., 2019b). The proposed approach requires the use of near zenith satellites. The height of the ionospheric inhomogeneity (HII) is delivered from the cross-correlation computation of two separately created maps of GNSS-detected disturbances (Fig. 24). The proposed method describes the characteristics of the ionospheric disturbances in the 4D space.

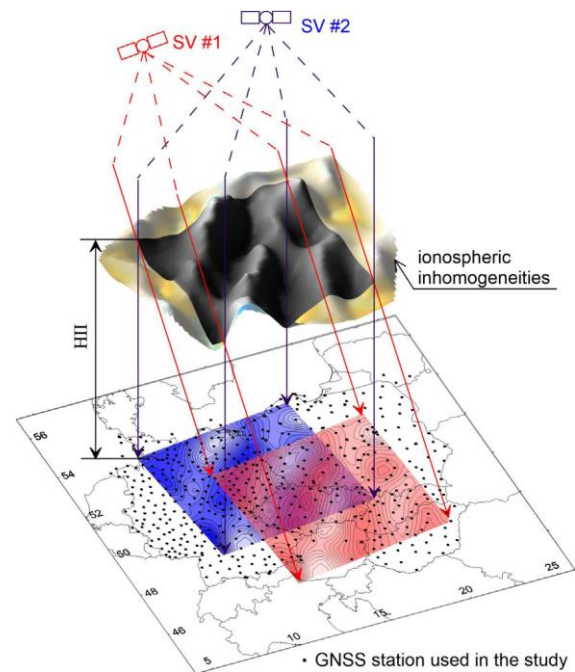


Fig. 24. Scheme of the idea of the height of ionospheric inhomogeneities (HII) estimation. Signals from two GNSS satellites (SV1 and SV2) are received by the dense network of GNSS stations (black dots). Based on the acquired observations, two independently ionospheric inhomogeneities maps are created (blue and red area). The correlation coefficients are calculated for the common area. The whole process is repeated for several heights of the ionospheric layer. The highest correlation coefficient corresponds to the actual HII

Analysed case study concerned a geomagnetic storm in March 2013. Results of the HII estimation have shown that during the quiet phase, when geomagnetic conditions tend to be calm, estimated HII are similar to those obtained from ionosondes (HII close to the height of F2 layer). In contrast to this, the active phase of a storm caused significant increasing of HII. This proved to be convergent with the changes of the slab ionospheric thickness and protons flux at the POES satellites orbit over Europe (Fig. 25).

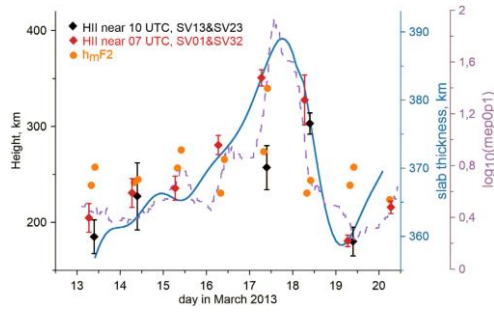


Fig. 25. Changes of the estimated height of the ionospheric inhomogeneities (HII) for the analysed period of time (13–20 March 2013). Red diamonds: the HII obtained near 07 UTC from the maps derived from SV01 and SV32. Black diamonds: the HII obtained near 10 UTC from the maps derived from SV13 and SV23. As a comparison the slab thickness of ionosphere (blue solid line), the logarithm of the intensity of protons flux (mep0p1) at the POES satellites orbit over Europe (magenta dashed line), and $h_m F_2$ for corresponding epochs (orange circles) are shown

Poniatowski and Nykiel (2020) presented the degradation of GNSS PPP solutions caused by the traveling ionospheric disturbances (TIDs) during the geomagnetic storm on 17 March 2015. The position root mean square (RMS) values during the storm reached up to several dozens of centimetres. They were significantly higher than the values obtained on a quiet day. Moreover, for some epochs, determination of the receivers position was impossible. This was due to the sudden decrease of the number of satellites used for positioning. They were excluded mainly because of the cycle-slip effects which frequently occurred for various satellites. It was proved that their occurrence was a result of the TIDs passage above the analysed GNSS stations.

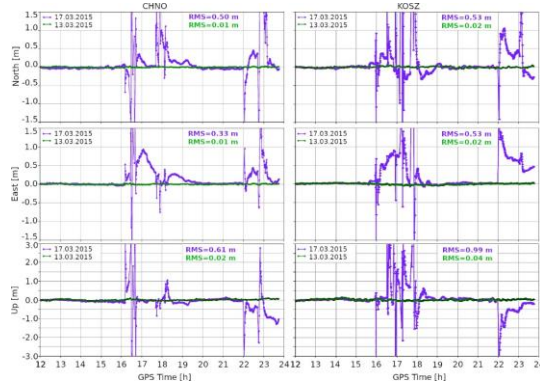


Fig. 26. Topocentric coordinates for the quiet (13 March 2015, the green line) and the stormy (17 March 2015, the magenta line) days; the example for the ASG-EUPOS reference stations CHNO and KOSZ

Figure 26 presents example results of topocentric coordinates for stormy (17 March 2015) and quiet (13 March 2015) days. The impact of the TIDs on coordinates accuracy is clearly visible between 16–19 UTC and after 22 UTC. On 17 March, the RMS

values for CHNO station (ASG-EUPOS network) were 0.50, 0.32, and 0.63 m for North, East, and Up components, respectively, whereas for KOSZ they were 0.53, 0.53, and 0.99 m. It is significantly higher in comparison to quiet days when these values are at the level of a few centimetres.

3.6. GNSS receiver antenna calibration

One of the crucial source of biases in GNSS measurements are the phase centre variations of the both transmitter and receiver antennae. For high-end applications based on carrier phase measurements, a set of consistent absolute phase centre corrections is necessary. So far absolute field calibration models were created for GPS L1 and L2 and GLONASS. Beside GPS and GLONASS, two additional systems are approaching full operational capability. The European Union (EU) with European Space Agency (ESA) introduce the Galileo positioning system. China has been developing the BeiDou system. Additionally, the current satellite navigation systems evolve into new modernized forms. Modernized GPS and GLONASS bring new signals. The modern GNSS satellites will broadcast at least three civil signals in a multiplicity of frequency bands.

The new GNSS systems together with GPS and GLONASS modernization cause the necessity to perform calibrations of receiver antennae designed for the new signals. Therefore, ASTRI Polska in cooperation with the UWM in Olsztyn started in 2019 the GRAVER project founded by the ESA. The purpose of the project is the development and implementation of field calibration procedure for multi-frequency and multi-system GNSS antennae (Dawidowicz et al., 2019a, 2019b; Krzan et al., 2020). The works on the project are in progress.

The preliminary results obtained show good agreement in comparison to the International GNSS Service (IGS) type-mean PCC values (Fig. 27). Calibration results for GPS L1 frequency of example antennae are very promising. For high elevations (20° – 90°) differences do not exceed 1.5 mm, while for low elevations (0° – 20°) the agreement of the results is worse, and differences exceeded 3 mm level for some antenna hemisphere region corrections.

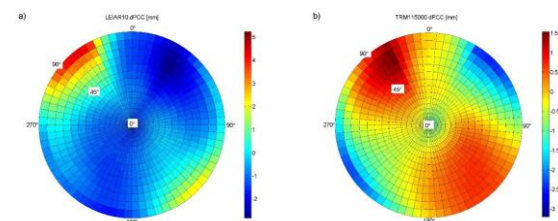


Fig. 27. Differences of derived full PCVs (GPS L1 frequency) between the final PCCs model and IGS calibration values for LEIAR10/NONE (left) and TRM115000.00/NONE (right) antennae

Cellmer et al. (2021) proposed substantial improvement in an ambiguity function-based GNSS precise positioning. The ambiguity function-based method's search procedure conducts in the 3D coordinate space, so the computational complexity, in this case, is independent of satellites' number. This property has a great importance due to the increasing number of satellites available for precise positioning. A new method of estimating the search step's length, determined by the actual satellite configuration was proposed. The data-driven search step estimated is always optimum, regardless of the current satellite configuration.

Research on the influence of antenna phase centre modelling on the determined positions was conducted at MUT. In particular, individual or type mean calibration tables were considered in terms of better results in height estimation. Araszkiewicz et al., (2019) discussed the differences between models and their impact on resulting heights. Analyses showed that, in terms of the stability of the determined height, as well as its variability caused by increasing the facade mask, both models gave very similar results. The impact of applying corrections dedicated to GPS frequencies to Galileo frequencies in the absence of the correct ones was also investigated (Araszkiewicz and Kiliszek, 2020). The results for both the absolute and relative positioning methods are clear: the use of GPS L2 corrections for the Galileo E5a frequencies results in a deviation of the estimated height of almost 8 mm (Fig. 28).

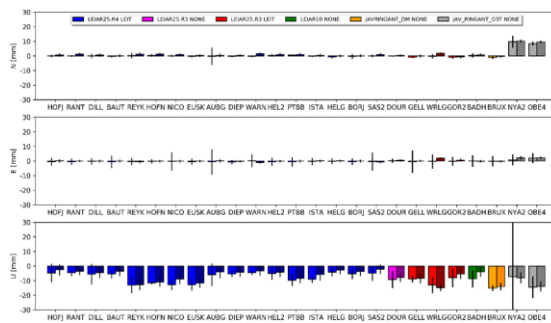


Fig. 28. Impact of using G2 (GPS) corrections for E5a frequencies (Galileo); darker columns refer to the DD approach

4. Advanced methods for satellite positioning

This section summarizes the studies conducted at UWM, devoted to GNSS processing algorithms development. The specific goals were related to the multi-constellation and high-rate signal processing as well as the application of smartphone GNSS observables to precise positioning.

A milestone on the way to the application of smartphones to location-based services was making in 2016 GNSS observations derived from the

devices running the Android Nougat 7 operating system accessible to all users. Since then it has been feasible to acquire raw pseudoranges, phase and Doppler observations. Related studies have been also conducted at UWM. Paziewski et al. (2019a) focused on challenging case, which is the application of low-power consumption smartphones which are the subject of duty-cycling mode. The specific objectives of this work were: the evaluation of smartphone observables with particular emphasis on anomalies present in phase and code observables driven by the duty-cycling mode as well as the performance assessment of the medium to long-range code-based relative positioning. The detailed results showed that in the case of smartphone GNSS positioning the C/N0-dependent weighting scheme was superior to the satellite-elevation one.

Paziewski (2020) offers a review of the most recent advances in smartphone GNSS positioning and applications as well as an outline of possible future developments. In the light of the recent advances, continuous progress in hardware, algorithms and applications is thought to be maintained in the future. With this development, the presumption of low-performance commonly related to low-cost receivers and smartphones may not hold true, since in the near future such receivers may potentially reach the performance level close to high-grade receivers.

Taking advantage of the advances in processing algorithms and the observation collection hardware, GNSS technology is nowadays commonly employed for seismic and geohazard studies. Paziewski et al. (2019b) contributed to the subject by presenting the result of the application of 100 Hz multi-constellation GNSS measurements. An enhanced Precise Point Positioning method was demonstrated and the performance by the application of shake table was validated. The experiment results confirmed a high applicability of the enhanced processing strategy to precise dynamic displacement detection. Specifically, it was achievable to characterize the amplitude of the dynamic displacements with precision at the level of millimetres. Paziewski et al. (2020) presented and validated the system developed for an automatic Galileo + GPS high-rate signals processing over medium-length baselines. The system aims at the detection of the displacement response to seismic events that are caused by mining exploitation. The system takes advantage of an ionosphere-weighted positioning model and a multi-station solution, which may be considered superior with respect to the commonly employed single-baseline mode. The results of the system validation with the data collected during actual MW 3.8 seismic event showed a high agreement between the GNSS and accelerometer-derived results in a frequency domain.

The simulated scenario experiment proved that the system is capable of detecting the dynamic displacements with a precision at millimetre-level at distances of over 30 km from reference stations.

Paziewski and Sieradzki (2020) presented and assessed the methodology that aims precise wide-area RTK and static relative positioning in the presence of severe ionospheric conditions. The approach takes advantage of multi-constellation network ionospheric corrections and an algorithm that eliminates the temporal variations of the ionospheric delays. The results of the experiment conducted during high-ionospheric activity demonstrated a very distinctive improvement in the ambiguity resolution domain and thus proved the advantage of the proposed approach over routine models such as ionosphere-float and ionosphere-weighted ones.

The analysis conducted so far concerning the determination of the PPP accuracy focused mainly on the results obtained from long (daily) static observation. The results obtained from the sub-daily observation, less often analysed, involved longer time intervals (1–8 h). In Dawidowicz (2019), time series of position components derived from sub-hourly (30 min) PPP solutions were analysed. The analysis was based on 30 days of observations performed at 8 ASG-EUPOS system stations. For processing the collected GNSS observations (in different variants) the NAVigation Package for Earth Orbiting Satellites (NAPEOS) software was applied. Assuming that standard deviation (SD) are a good measure of the accuracy of the obtained results, the conducted analyses prove that the sub-hourly PPP technique can provide accuracy at the level of 0.5 cm for the horizontal position components and 1 cm for the vertical position component. The above accuracy was obtained in the multi-station PPP approach (fixed ambiguity solution). In float ambiguity solution scenarios, the SD increases up to 1 cm for horizontal components and up to 2 cm for the vertical component. The periodicity, in the obtained position components time series were analysed using the Lomb-Scargle periodogram. Spectral analysis showed clear periodicity in the obtained results (especially for GPS-only fixed and float solutions). For GPS or GPS/GLONASS processing strategies 73% of detected periodic signals correspond to a multiple of the orbital periods of the satellites.

UWM in Olsztyn was a Prime Contractor in the COSTO (Contribution Of Swarm data to the prompt detection of Tsunamis and Other natural hazards) project, which has involved the National Observatory of Athens (NOA), Technical University of Munich (TUM/DGFI-TUM) and Technical University of Catalonia (UPC/UPC-IonSAT). The main objective of COSTO project was to better characterize, understand and discover

coupling processes and interactions between the ionosphere/magnetosphere, the lower atmosphere and the Earth's surface and sea level vertical displacements. The proposed research targets to the tsunamis that are the result of earthquakes (EQ), as well as to the ionospheric responses with respect to general seismic activity related with these events. The idea of COSTO study was based on the symbiosis of Swarm data, ground GNSS data and seismic records combined with the information on EQs and tsunamis. Swarm data processed with the use of the fast Fourier transform (FFT) is applied in the detection and preliminary classification of SIDs related with EQs and tsunamis (Jarmolowski et al., 2020), whereas ground GNSS data and seismic records help in their validation.

The largest tsunami that can be investigated by Swarm mission data is triggered by the $M_w = 8.3$ EQ, which is also one of the largest EQs in this period. This tsunami event took place on 16.09.2015, off the coast of central Chile, near Illapel. The seismic activity before and after the mainshock induces SIDs, which can be observed by Swarm and ground GNSS stations (Jarmolowski et al., 2021). An example of co-located Swarm pass and ground GNSS observations, at time of SID triggering is given in Figure 29. Different ionospheric anomalies were recorded along Swarm satellite orbits located over EQ/tsunami events at the time of these events, or closely to them in time and space, when a related seismic activity takes place. The classification of the spectral characteristics of disturbing along-track signals is supported by their simultaneous search in ground GNSS observations, which gives an opportunity for the validation of the spectral recognition. Filtered disturbing signals from Swarm and ground GNSS, which are observable in the same place and time, can be analysed together. STFT spectrograms can be made for the selected Swarm along-track data samples (Fig. 29a), whereas keograms and scatter plotting can be done for ground GNSS carrier phase LG-F (geometry-free combination) data (Fig. 29b). This way the SIDs observed by Swarm can have determined their individual spectral patterns, whereas GNSS observations from dense ground networks can be used for the validation purpose, by the analysis of SID's spatiotemporal correlation.

STFT spectral approach to along-track Swarm data studied in the frame of COSTO gives an opportunity for distinguishing the signals of different origin. The COSTO studies open a way to analyse the system of seismically induced ionosphere anomalies for a wider range, including also internal validation of the observed anomalous signals. The COSTO research outcomes can constitute a basis of a prototype solution for investigating solid Earth-atmosphere-ionosphere coupling. The symbiosis of local ground GNSS

networks with Swarm satellite observations extends the coverage of SIDs detection system from local to global. Ground GNSS data validates Swarm, whereas Swarm extends the range of sensing and recognizes SIDs spectrally.

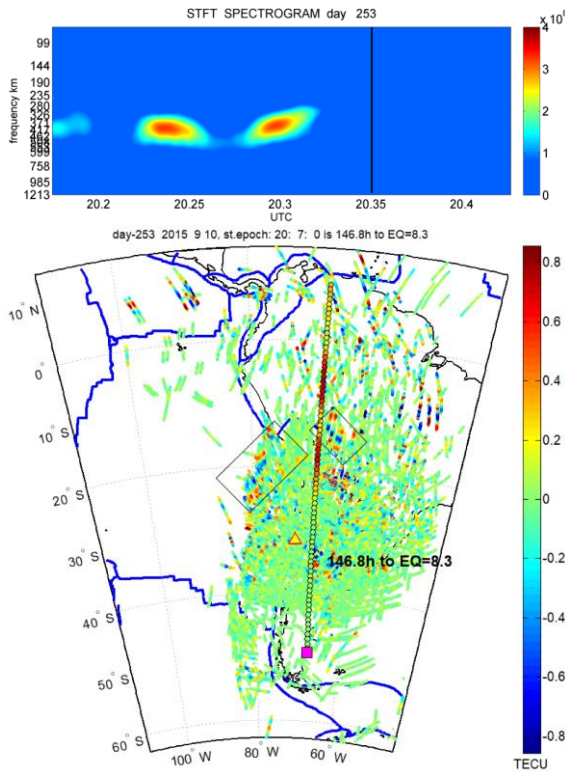


Fig. 29. Example of co-located Swarm pass and ground GNSS observations, at time of SID triggering

Another study carried out at UWM concerned accuracy analysis of global ionosphere maps (GIMs) provided by Ionosphere Associate Analysis Centers (IAACs) of the International GNSS Service (IGS). In this study, the accuracy and consistency of the IAAC GIMs during high (2014) and low (2018) solar activity periods of the 24th solar cycle was evaluated. The GIM-derived slant TEC (STEC) was compared to carrier phase geometry-free combination of GNSS signals obtained from 25 globally distributed stations. A good consistency between different GIMs was observed (Fig. 30). The highest accuracy level was obtained for UQRG maps, which may indicate some advantage of the stochastic approach (kriging). From the IAAC GIMs, usually the best results were obtained with the CODG product.

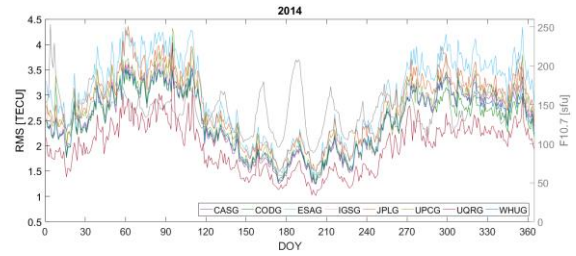


Fig. 30. F10.7 index and daily RMS distribution based on a comparison with ground GNSS observations for all analysed GIMs in 2014

Quality control of GNSS data processing using information criteria

The quality control of GNSS data processing can be divided into two parts. The former is the validation of so-called underlying functional model and the latter is the quality description of final model parameter estimates. The underlying functional models are validated using statistical hypothesis testing – usually by so-called DIA testing procedure – to detect, identify and adapt (parametrize) possible faults. Since the DIA procedure is not mathematically rigorous and optimum under multiple faults in underlying model, Nowel et al. (2020) adapted and discussed the information criterion (IC) approach for the validation of baseline GNSS functional models. Three IC methods were compared with the conventional DIA procedure. To verify the reliability of the two considered approaches, several scenarios differing in: the magnitude and number of faults, and the interval between measurement epochs were investigated. Generally, the DIA procedure achieved the highest rates of correct model specification when no fault existed. However, as the number of faults was increasing one of the IC methods was starting to achieve the highest rates.

The performance of Galileo-only absolute positioning using dual-frequency observations was evaluated and compared to the performance of GPS-only positioning (Hadas et al., 2019). Standard Point Positioning (SPP) using pseudoranges and PPP with pseudoranges and carrier phase observations, both using broadcast (B), real-time (R) and MGEX Final (M) orbits and clocks were performed in the static and kinematic mode for 20 IGS stations. Although only 22 Galileo and 32 GPS satellites are useful for real-time solutions, Galileo outperformed GPS in several variants (Fig. 31), i.e. in the classical SPP mode (SPP+B) and PPP based on broadcast ephemeris (PPP+B).

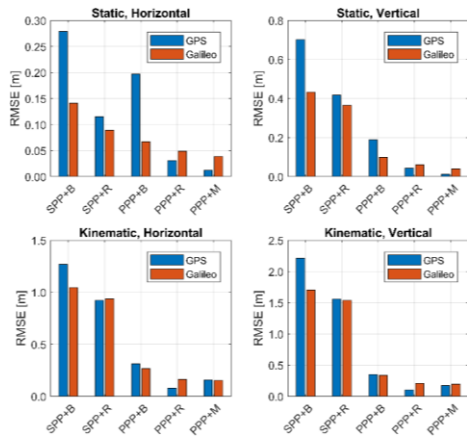


Fig. 31. RMSE between coordinates estimated with GPS and Galileo in five different variants and IGS weekly combined solution (SPP-single point positioning, PPP-precise point positioning, B-broadcast ephemeris, R-real-time service products, M – IGS MGEX Final products)

In particular, the accuracy of Galileo-only PPP+B was 7 and 10 cm, for the horizontal and vertical component, respectively, which is superior to the corresponding GPS-only solutions by the factor of 3 and 2, respectively. This confirms the superior quality of Galileo pseudoranges, the high accuracy of broadcast orbits and stability of Galileo onboard clocks. On the other hand, PPP with real-time (PPP+R) and final MGEX (PPP+M) products are still more accurate with GPS, especially in the static mode, so further improvement in the quality of Galileo products is required.

MUT team conducted research on the change of the performance of the PPP positioning with the development of GNSS systems (Kiliszek and Kroszczynski, 2020). The same software, model and products were applied for processing data from three different periods in 2017-2019 for different combinations of GPS, GLONASS and Galileo systems and for different elevation angles from 0° to 40° (simulating different observation conditions). The results of analysis showed that the highest accuracy and the shortest convergence time which were obtained in 2019 using all three systems together. The development of the Galileo system had a particular impact on the improvement of the results obtained, but the GPS system still had the greatest impact on the accuracy of multi-GNSS positioning. The use of only Galileo system allows for positioning anywhere on Earth and the results obtained in 2019 are of 50% better than those in 2017. Using all three GNSS systems together also enables positioning with high accuracy for the higher elevation angles; about 90% availability of solutions with centimetre accuracy of position for 40° elevation angle can be achieved. It was shown that the Galileo had improved more with years but it is still provides worse results than GPS and GLONASS together.

5. Improving consistency between SLR and GNSS solutions

5.1. The Blue-Sky effect

The Blue-Sky effect has been assessed based on SLR observations to multi-GNSS satellites. This effect limits the consistency between laser techniques in satellite geodesy (SLR) and microwave techniques (GNSS, VLBI) due to the fact that SLR observations are conducted during good weather conditions (clear sky) when the surface of the Earth is deformed by high atmospheric pressure (Atmospheric Pressure Loading). The geophysical Blue-Sky effect was first estimated for all SLR laser stations conducting observations to LAGEOS geodetic satellites, and more recently also for laser stations performing measurements to GNSS satellites. The use of SLR observation to GNSS satellites was possible thanks to intense ILRS tracking campaigns and a significant increase in laser tracking of the new GNSS satellites. The method of determining the size of the Blue-Sky effect with the determination of the effect in observations for geodetic and GNSS satellites is described (Bury et al., 2019a).

5.2. IGS activities and processing of SLR observations to GNSS satellites

Precise orbit determination of new GNSS systems constitutes one of the major research topics at WUELS. For the Galileo system, the satellite metadata have been released with the details on the absorption, reflection, and dispersion coefficients for all satellite surfaces. These parameters allow for the composition of the box-wing models (Bury et al., 2020). A series of tests has been conducted incorporating pure box-wing solutions, empirical solutions using different versions of the Empirical CODE Orbit Models (ECOM), and hybrid solutions based both on empirical and box-wing models (Bury et al., 2019c). Moreover, the methodology of multi-GNSS orbit determination using SLR was developed and described by Bury et al. (2019b).

The International GNSS Service (IGS) launched in 2019 an experimental combination of multi-GNSS orbits based on products delivered by the Multi-GNSS Experiment Pilot Project (MGEX)¹⁵. The experimental IGS combined orbits that include GPS, Galileo, GLONASS, BeiDou-2, BeiDou-3, and QZSS systems, have been validated with a comprehensive quality assessment of the derived products (Fig. 32). The methodology of deriving combined IGS orbits and the results of the quality evaluation were published (Sosnica et al., 2020).

¹⁵http://acc.igs.org/mgex_experimental.html

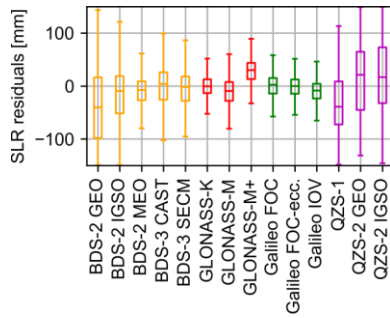


Fig. 32. Quality of experimental multi-GNSS IGS orbits validated using SLR observations

Kaźmierski et al. (2020) evaluated the quality of real-time satellite orbits and clocks in terms of the Signal-in-Space-Ranging-Errors (SISRE) with a distinction between the orbital and total SISRE. The authors found a substantial improvement of the quality of Galileo products over time, which give today even more precise total SISRE values than the GPS system. Galileo benefits from high-stability onboard clocks which guarantee the superior accuracy of Galileo-based products and reduce the periodical radial orbit errors.

5.3. Processing SLR observations to Low Earth Orbiters (LEO) for a GNSS-SLR integration onboard satellites

One of the fundamental elements limiting the accuracy of laser measurements are hardware and system biases (range biases), which depend on the type of detector at the SLR stations, power and length of the laser pulse, delays in the system circuits, laser wavelength, type of retroreflector and the number of corner cubes in the retroreflector array onboard the satellite). Neglecting range biases leads to significant systematic errors, especially when laser measurements are used to validate low or high satellite orbits (Strugarek et al., 2019a; 2019b; Arnold et al., 2019).

An empirical method has been proposed to reduce the impact of range biases by estimating corrections to station coordinates and estimating biases for long time series (minimum 1 year) and re-substitution of estimated biases, alternatively also station coordinates in epoch solutions (e.g. 1-day). The method functions both for stations affected by biases and stations that have incorrect coordinates in the a priori reference frame. For example, as a result of applying corrections of standard deviations of laser observations to the orbit of the Sentinel-3A satellite determined using GPS observations, the corrections decreased residuals from 12.4 to 8.6 mm, which is 30% (Fig. 33). The method improves the quality of SLR solutions using observations of LEO satellites (Strugarek et al., 2019a; 2019b) as well as SLR observations to GNSS satellites (Sosnica et al., 2019).

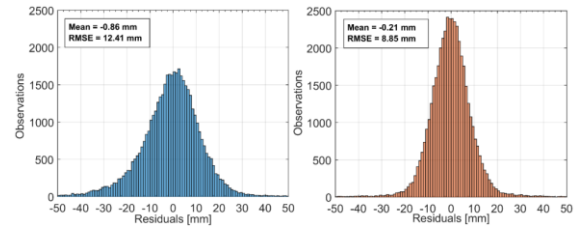


Fig. 33. Distribution of laser observation residuals to the microwave orbits of the Sentinel-3A satellite without (left) and after (right) taking into account the reduction of range biases and corrections to station coordinates for all SLR stations in 2016

5.4. Tropospheric delay model for SLR and improving the consistency between SLR and GNSS

In order to improve modelling of the tropospheric delay in laser observations and to improve the consistency between SLR and GNSS, the currently used model was extended with horizontal gradients that account for the asymmetry of the tropospheric state above laser stations (Drozdowski et al., 2019) (Fig. 34).

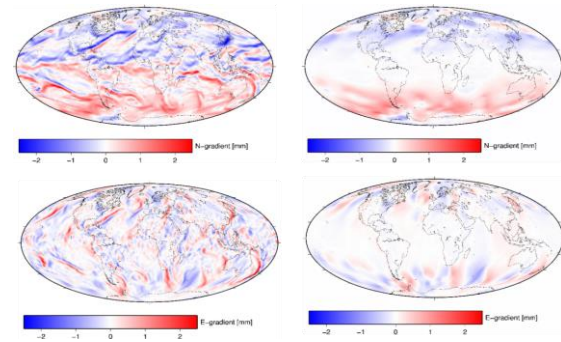


Fig. 34. Horizontal gradients of the tropospheric delay: northern (top) and eastern (bottom) in GNSS microwave observations (left) and SLR laser observations (right) for 1 January 2016, 0:00 based on numerical weather models

6. GNSS for navigation

The InnoSatTrack research project of GUT and Gdynia Maritime University is focused on the examination of the possibility of improving the accuracy of geometric parameters of a railway track with a specific number of GNSS receivers. Improvement of the GPS and GLONASS systems accuracy, construction of new systems (Galileo/BeiDou), and creation of new multi-constellation geodetic GNSS systems have contributed to the rapid development of the method. Previous studies conducted in 2009–2017 in two main directions: geodetic – associated with increasing the measurement accuracy and availability (Specht et al., 2019) were related to the device construction – aimed at developing new design and operation methods.

Four railway measurement campaigns were carried out, with the use of high-frequency (20 Hz and 100 Hz) GNSS receivers, mobile laser scanner, INS devices, inclinometers, and vision cameras. The number of sensors installed on a mobile railway measuring platform (Fig. 35) required the development of a methodology for appropriate synchronous processing of the collected measurement data with least squares method (Czaplewski et al., 2020). The first results are published (Wilk et al., 2020a; Wilk et al., 2020b; Specht et al., 2020).

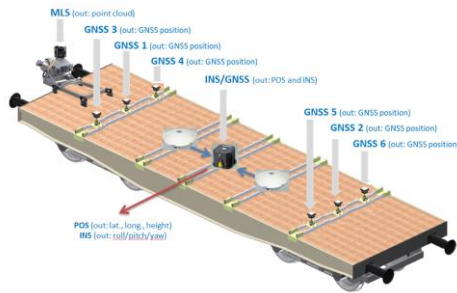


Fig. 35. Mobile railway platform with sensors installed during the campaign in Kłosnowo

The method proposed in the InnoSatTrack research project is based on both kinematic real-time and post-processing GNSS measurements. It uses a typical 4-axis freight wagon platform equipped with several GNSS receivers placed in the fixed frame. Two receivers are installed above the pivot pins of the two bogies that theoretically continuously indicate the track axis. According to that, the real position of the railway track axis during the wagon motion is obtained. The study (Wilk et al., 2021) proposes an innovative method to determine the railway track axis based on the geometric constraint called the fixed base.

7. ASG-EUPOS network

7.1. Status of the ASG-EUPOS network

After implementation of Galileo and BeiDou signals into real time services of ASG-EUPOS system operated by GUGiK, further minor upgrades were performed in 2019. The automatic post-processing module was upgraded, to be ready to provide multi GNSS (GPS/GLONASS) automatic post-processing calculations, and the GNSS data stored in RINEX 3.xx format.

In 2019 12 additional reference stations were upgraded to track 4 GNSS systems. Also 12 new choke ring antennae with individual GPS+GLO+GAL+BDS calibrations were installed.

After upgrades conducted in 2017-2019, the ASG-EUPOS System provides services based on 4 GNSS constellations: GPS+GLO+GAL+BDS. Even if single station is not capable to track 4 GNSS

systems, RTN correction data including Galileo and BeiDou are distributed over the whole country.

At present 125 permanent reference stations operate within the ASG-EUPOS network (118 of 4GNSS: GPS+GLO+GAL+BDS, 1 of 3GNSS:GPS+GLO+GAL, and 6 of 2GNSS: GPS+GLO) (Fig. 36).



Fig. 36. Reference stations of the ASG-EUPOS system (March 2021)

The densification of the reference network has been undertaken to increase availability and accuracy of real time services. The additional new reference stations are planned to be established in 2021–2023.

In cooperation with the Military University of Technology, GUGiK participates in the EPN Densification project¹⁶ (Kenyeres et al., 2019). The new EPND release (D2100) includes ASG-EUPOS solutions up to GPS week 2100 (11-04-2020). As part of the EPN Densification project MUT provides also solutions for ASG-EUPOS network. It is a Polish contribution to the continental-scale (European), homogeneous position and velocity for a dense network of GNSS stations. This solutions is used by both EUREF working group on "Deformation models" and EUREF Working Group on "European Dense Velocities"¹⁷.

To support surveying, construction and agriculture companies in SARS-Cov2 pandemic period, the postprocessing services and decimetre level real time DGNS services are available free of charge. Some of this regulations in July 2020 became implemented permanently as changes in geodetic and cartographic act.

To secure stable and uninterrupted work for next years, IT components (servers and network hardware) in Management Centres are being exchanged step by step. The Management software

¹⁶http://www.epncb.oma.be/_densification/

¹⁷http://pnac.swisstopo.admin.ch/divers/dens_vel/index.html

for generating correction data was upgraded to the latest version which is better prepared to utilize BeiDou segment III signals.

8. Modelling precise geoid

Activities of the team of IGIK on the improvement of the accuracy of precise quasigeoid modelling for Poland were continued. New sets of gravity anomalies for the area of Poland, i.e. mean free-air anomalies of 5'×5' for the purpose of including them in the EGM2020 global geopotential model, and mean Faye anomalies of 1'×1' for modelling geoid for Poland, were generated. Gravity values from the detailed gravity survey as well ~1% of gravity stations from semi-detailed survey affected with gross errors were not included in the process of calculating these new sets of gravity anomalies. Moreover, more accurate formula for the free-air gravity gradient was applied instead of 0.3096 coefficient. Using the new set of 1'×1' mean Faye anomalies the new gravimetric quasigeoid model was developed. Standard deviations of differences between quasigeoid heights obtained from this model and from GNSS/levelling data do not exceed 2 cm (1.4–1.7 cm).

Gravimetric quasigeoid models GDQM-PL13 and GDQM-PL19 developed in the last years by the IGIK team were compared with the official Polish quasigeoid models¹⁸ called (1) gugik-geoid2011-PL-KRON86-NH that is based on the PL-KRON86-NH vertical reference frame, and (2) gugik-geoid2011-PL-EVRF2007-NH which is compatible with the PL-EVRF2007-NH vertical reference frame. The gugik-geoid2011-PL-KRON86-NH and gugik-geoid2011-PL-EVRF2007-NH models in 0.01°×0.01° grids were obtained by fitting height anomalies determined from the EGM2008 (Earth Gravitational Model 2008) Global Geopotential Model (GGM) into the corresponding ones determined using GNSS/levelling data from ASG-EUPOS (Active Geodetic Network of European Position Determination System; www.asgeupos.pl), EUREF-POL (EUropean REference Frame – POLand), POLREF (POLish REference Frame) and EUVN (EUropean Vertical Reference Network) networks. These quasigeoid models are obligatory for use in geodetic practice. The GDQM-PL13 and GDQM-PL19 quasigeoid models were developed using EGM2008, mean 1'×1' Faye gravity anomalies and deflections of the vertical for the area of Poland as well as free air gravity anomalies for territories surrounding Poland. The remove-compute-restore procedure and the least squares collocation method were utilized to develop these models. The main difference between the GDQM-PL13 and GDQM-PL19 quasigeoid models results from different sets of mean Faye anomalies used;

refined mean Faye anomalies were incorporated in the later quasigeoid model. Both GDQM-PL13 and GDQM-PL19 quasigeoid models are given in 1.5'×3' grids. Statistics of differences between height anomalies determined from gravimetric GDQM-PL13 and GDQM-PL19 models and the corresponding ones determined from fitted gugik-geoid2011-PL-KRON86-NH and gugik-geoid2011-PL-EVRF2007-NH models at IGIK's models grid points are given in Table 2.

Table 2. Statistics of differences between height anomalies determined from GDQM-PL13 and GDQM-PL19 models and the corresponding ones determined from gugik-geoid2011-PL-KRON86-NH and gugik-geoid2011-PL-EVRF2007-NH models [m]

Model	Min	Max	Mean	Std. dev.
GDQM-PL13 – KRON86	-0.276	0.130	-0.066	0.016
GDQM-PL19 – KRON86	-0.403	0.150	-0.089	0.015
GDQM-PL13 – EVRF2007	-0.111	0.295	0.100	0.014
GDQM-PL19 – EVRF2007	-0.238	0.315	0.076	0.014

Since the use of the PL-KRON86-NH vertical reference frame in Poland has been extended by the end of 2023, for next four years this frame will still officially be applied parallel to PL-EVRF2007-NH. The new reference surface for heights was developed using the current pl-geoid2011 model based on EGM2008, fitted to PL-KRON86-NH, and then corrected for differences between PL-KRON86-NH and PL-EVRF2007-NH heights. Those corrections are determined by means of Helmert's seven parameter transformation on the basis of over 35 000 benchmarks of the basic levelling network, common for both frames realization. The complicated procedure of calculation of geoid heights from the model as well as the level of errors induced into vertical networks encouraged the team of the Warsaw University of Technology to implement the reference surface for heights in Poland by using the European Gravimetric Geoid models. Gravimetric height anomalies determined on the basis of EGG2008 and EGG2015 models were compared with the respective ones from satellite/levelling data from the stations of the ASG-EUPOS network (Marjanska et al., 2019). Estimated fit of geoid undulations calculated from the EGG2015 model to satellite/levelling data is at the level of 2 cm. Fitting Using trigonometric polynomials that fit is reduced to 1.3 cm. The results of the next realizations of the EGG models might be better through sharing new gravimetric and satellite/levelling data from parts of the Polish territory to the National Geodetic Survey and the University of Leibnitz in Hannover.

¹⁸<http://www.gugik.gov.pl/bip/prawo/modele-danych>

Trojanowicz (2019) investigated the local quasigeoid modelling based on the geophysical gravity data inversion (GGI) method. The model includes information on density distribution, thus it can be considered as a local integrated model of both: the external gravity field and the density distribution of the Earth's crust. The performed calculations indicated a very high accuracy of the determined quasigeoid model which is developed when the modelling process includes the use of a GGM. Standard deviations of differences between height anomalies obtained from the model determined and from GNSS-levelling data are at the level of 1.5 cm.

Trojanowicz et al (2020a) focused on the modelling of local quasigeoid in South-Western Poland using precisely defined GNSS/levelling height anomalies at 9 stations, EGM2008, terrestrial gravity data and topography data. Four approaches: Least Squares Collocation (LSC) approach, Thin Plate Spline (TPS) approach, Integrated approach based on Molodensky's theory and the LSC, and

Geophysical Gravity data Inversion (GGI) approach, were compared with the EGM2008 (Fig. 37).

The EGM2008 was used in three versions: as the full model (up to degree 2190 and order 2159) and as the truncated model to a degree and order of 1000 and 360. The influence of distance between the points with known height anomalies was also investigated. 9 sets of GNSS/levelling points ranging from 10 to 90 were considered. The standard deviation of the differences $\delta\zeta_{mod} = \zeta_{GNSS/lev} - \zeta_{mod}$, where ζ_{mod} is the height anomaly obtained from the model, was used as the basic accuracy characteristics (Fig. 37). Figure 37a presents values for three versions of maximal degree and order of EGM2008. Figures 37b and 37c present values for various number of known GNSS/levelling points for EGM2008 in versions: $N_{max} = 2190$ (Fig. 37b) and $N_{max} = 360$ (Fig. 37c).

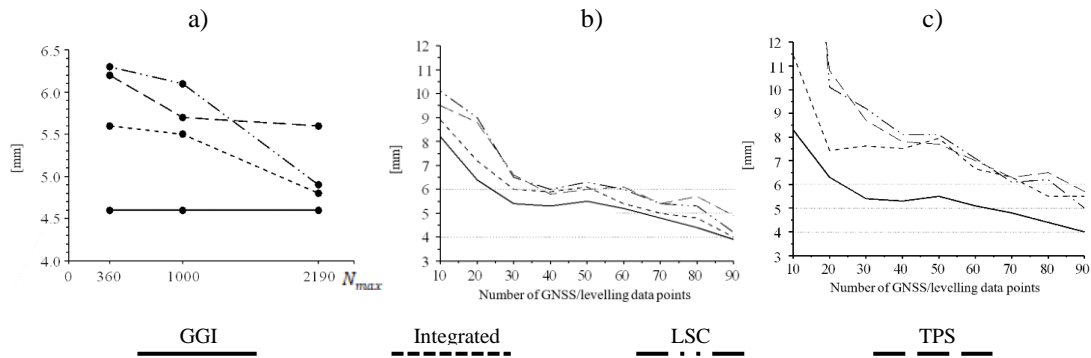


Fig. 37. Standard deviations of differences between height anomalies obtained using 4 approaches and the corresponding ones from the EGM2008; (a) N_{max} (360, 1000, 2190), (b) $N_{max} = 2190$ and (c) $N_{max} = 360$

The authors conclude that for a dense network of GNSS/levelling points (about 1 point per 30 km²), there is no explicit need for using advanced quasigeoid modelling methods employing gravity data. It is entirely sufficient to apply the known interpolation methods available in many popular spatial data modelling programs. The differences between the modelling results became significant only with an increase in the distance between the GNSS/levelling data points and the reduced accuracy of the GGM applied.

The latest global density model of topographical masses (UNB_TopoDens model) was used to determine complete Bouguer anomalies and differences between geoid undulations and height anomalies in an area of the Western Carpathians within the Polish-Slovak-Czech border region.

The maps of determined values are presented in Figure 38 (complete Bouguer anomalies) and Figure 39 ($(N - \zeta)_{UNB}$ differences).

The results show significant differences due to the various densities adopted for the calculations.

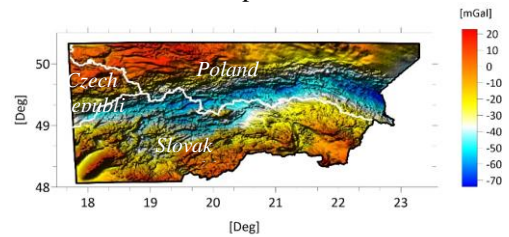


Fig. 38 Map of the complete Bouguer anomalies CBA_{UNB}.

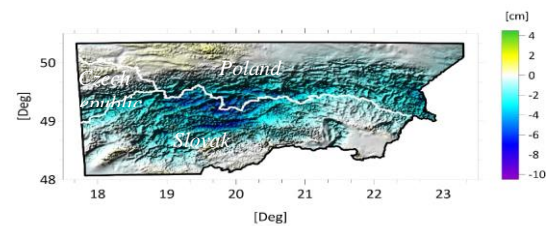


Fig. 39. Map of the differences $(N - \zeta)_{UNB}$

For example, differences between the Bouguer anomalies as well as height anomalies obtained using densities from the UNB_TopoDens model and those using a constant density of 2670 kg/m³ range from -3.4 mGal to +37.5 mGal, and from -0.5 cm to +7.4 cm respectively. It was also shown that for high mountain areas differences between geoid and quasigeoid heights should be determined on the basis of exact formula, not on the basis of Bouguer anomalies (Trojanowicz et al., 2020b).

The properties of the GGI model as the more universal disturbing potential model were analysed by Trojanowicz et al. (2020c). The investigations were performed in the area of the Western Carpathians covering the Polish–Slovak border. A detailed assessment of the model's properties was made regarding the accuracy of the disturbing potential values (height anomalies), gravity values, complete Bouguer anomalies (CBA), and differences between geoid undulations and height anomalies ($N - \zeta$). Available geoid models from Poland and Slovakia areas were used in the analyses. Obtained accuracies of the GGI quasigeoid model (in terms of standard deviation of the residuals to the reference quasigeoid models) were at the level of ± 2.2 cm for Poland and ± 0.9 cm for Slovakia area, which means a better fit of the GGI model to the quasigeoid model of Slovakia. There were also shown dependence of the accuracy of gravity prediction by the GGI method on the digital elevation model (DEM) resolution, the point height, the density of gravity data used as known data and used reference density model of topography. The best obtained accuracy of gravity prediction by GGI method were at the level of ± 1 mGal. The GGI approach was compared with classical gravity prediction methods (using CBA and topographic-isostatic anomalies supported by Kriging prediction), getting very similar results. In terms of CBA determined by the GGI method, it was noted the strong dependence of the resolution of this values on the size of the constant density zones of GGI model, which significantly reduces the quality of the determined CBA values. Dabrowski (2019) from the Gdynia Maritime University investigated on the territory of Poland the accuracy of GGMs used in Smartphone positioning. Comparative analysis between geoid heights obtained from seven geoid models implemented in different smartphones and the EGM2008 was presented. The overall results reveal that the EGM2008 provided highly accurate reference geoid undulation values along the measured profiles and locations.

Estimation of sea level changes

Absolute sea level changes at the tide gauge station in Wladyslawowo on the Polish coast of the Baltic Sea were estimated using GNSS and tide gauge data with different time series software packages:

Hector, GITSA, GGMatlab, and Statistica (Lyszkowicz and Bernatowicz, 2018). The authors indicated the Hector software package as most recommended.

Geocentric changes in the Baltic Sea level along southern coast, i.e. changes referred to the origin of the ITRF were investigated (Lyszkowicz and Bernatowicz, 2018) to fill the gap in the SONEL network that monitors the level changes of the Baltic Sea. The trend, annual and semi-annual terms were calculated for GNSS and tide gauge series for six stations: Hel, Wladyslawowo, Leba, Ustka, Kolobrzeg, Swinoujscie. At five stations investigated the trend estimated is at the level of 3 mm/year except Ustka where it reaches the value of 4.68 mm/year.

9. The use of data from satellite gravity missions

Validation of the newest GGMs

The quality of the newest GGMs was investigated by the team of IGiK. The latest official GGMs of the GOCE satellite mission, i.e. release 6 of GOCE-based GGMs, such as GO_CONS_GCF_2_TIM_R6 and GO_CONS_GCF_2_DIR_R6 which are satellite-only GGMs, GO_CONS_GCF_2_TIM_R6e model for which developing terrestrial, marine and airborne gravity data for polar areas besides GOCE data were used as well as the combined XGM2019e model of very high resolution up to 5540 degree/order, were validated. The validation was based on the comparison of height anomalies obtained from these models with the corresponding ones obtained from ASG-EUPOS GNSS/levelling data. The release 6 of GOCE-based GGMs seems slightly better (i.e. 1–3 mm in terms of standard deviation of the differences) than the previous one, i.e. RL05 GOCE-based GGMs. The improvement of fitting the XGM2019e model truncated at degree and order (d/o) 2190 to GNSS/levelling data comparing to the fit of EGM2008 and SGG_UGM_1 models to these GNSS/levelling data was not observed.

The combined XGM2019e Global Geopotential model of very high resolution up to 5540 degree/order (d/o) was validated over the area of Poland. Its validation was based on the comparison of gravity anomalies obtained from this GGM using GrafLab (GRAvity Field LABoratory) software with the corresponding ones obtained from a set of highly accurate absolute gravity data at 161 gravity stations of the modernized Polish gravity control network. In order to compute fully normalized associated Legendre functions at ultra-high d/o, the extended-range arithmetic algorithm was applied. The short-term gravity signal beyond d/o 5540 was compensated using the SRTM30 (Shuttle Radar Topography Mission 30"×30" model. The results obtained indicate the accuracy of 3.84 mGal of the

XGM2019e over the area of Poland which is approximately twice lower than the accuracy of the EGM2008. The main reason of this can be ascribed to the fact that the XGM2019e was developed using terrestrial gravity data of 15'×15' spatial resolution, while very accurate terrestrial gravity data of 5'×5' spatial resolution were utilized to develop the EGM2008.

Determination of temporal variations of geopotential functionals using the latest products from gravity satellite missions

In 2019, level 2 products of GRACE-FO satellite mission were delivered to the community. They were developed by computational centres of the mission according the same standards as in the case of the latest release, i.e. release 6 (RL06), of GRACE-based GGMs, and thus, they are also called RL06. Using these data, i.e. RL06 GRACE/GRACE-FO-based GGMs, temporal variations of geoid heights for the area of Poland were calculated. The IGIK–TVGMF (Institute of Geodesy and Cartography–Temporal Variations Gravity/Mass Functionals) software was utilized (Godah, 2019). The RL06 GRACE/GRACE-FO-based GGMs used were filtered with the DDK3 filter and truncated at d/o 60. Time series of geoid height changes determined for the area of Poland with the use of GRACE/GRACE-FO-based GGMs are shown in Figure 40.

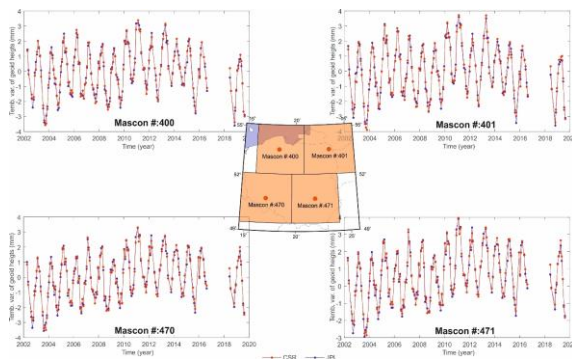


Fig. 40. Geoid height variations for the area of Poland obtained from release 6 of GRACE/GRACE-FO-based GGMs

The location of the areas for which the time series of geoid height variations were determined coincides with the location of mascons which are other type of product of the GRACE satellite mission and in the near future they will be the product of GRACE-FO. Differences between temporal variations of geoid height for the area of Poland obtained from GRACE satellite mission data in CSR (Center for Space Research at University of Texas, Austin) and JPL (Jet Propulsion Laboratory) computational centres reach 0.5 mm at the beginning of the mission, i.e. in 2002, but in the rest of the period investigated they do not exceed

0.2 mm. In the case of the GRACE-FO satellite mission the time series determined are almost identical, the differences between them do not exceed 0.1 mm. Also the recovery of temporal variations of geoid heights determined with the use of GGMs based on SST-hl data from non-dedicated gravity satellite missions was investigated (Godah et al., 2019e).

Research on temporal variations of geoid heights ΔN for the area of Poland from monthly GGMs developed using GRACE-FO satellite mission data (i.e. release 6 (RL06) GRACE-FO-based GGMs) was continued in 2020 with the use of the IGIK–TVGMF software, following the strategy applied in 2019. Time series of ΔN over Poland determined from CSR and JPL GRACE-FO-based GGMs (Fig. 41) are quite similar, as standard deviations of the differences between the corresponding ΔN determined from CSR and JPL GRACE-FO-based GGMs do not exceed 0.4 mm.

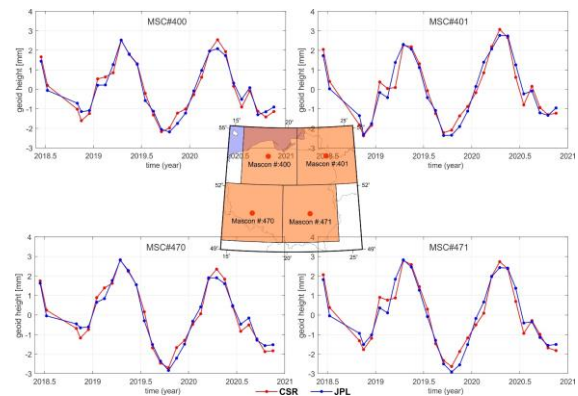


Fig. 41. Temporal variations of geoid heights for Poland obtained from RL06 GRACE-FO-based GGMs

Accuracy of gravity field changes from GRACE RL06 and RL05 data compared to in situ gravimetric measurements were analysed in the context of choosing optimum filtering type analysis (Szabó and Marjanska, 2020).

Contribution of gravity satellite missions to the Earth's gravity field modelling – research for areas of Ethiopia and Uganda in the Eastern Africa

Investigations concerning the contribution of gravity satellite missions to modelling gravity field for the area of Ethiopia and Uganda in East Africa were conducted (Godah et al., 2018, Godah et al., 2019a). Geopotential functionals, i.e. the gravity disturbance and quasigeoid height, were determined from four combined GGMs, namely: EGM2008, Eigen-6C4, GECO and SGG-UGM-1, and seven satellite-only GGMs namely: SPW_R5, DIR_R5, TIM_R5, IfE_GOCE05s, NULP_02s, IGGT_R1 and GOSG01S. Then the gravity disturbance and quasigeoid height determined were compared with

airborne/terrestrial gravity data available for the area of Ethiopia and GNSS/levelling data available for the area of Uganda. The omitted gravity signal in satellite-only GGMs was compensated with the EGM2008 using its spherical coefficients from the applied maximum degree to 2190 degree/order. The main findings reveal an improvement of ca. 40–50% on the modelled gravity field from GGMs that include data from GOCE satellite mission. For the area of Uganda the best fit, i.e. 14 cm, was obtained for SGG-UGM-1 combined model as well as IGGT_R1 GGM truncated at d/o 200. For the area of Ethiopia the best fit, i.e. 1.9 mGal, was observed for the NULP_02s GGM truncated at d/o 200. The worst fit was obtained for EGM2008 model, 3.9 mGal and 27 cm, for Ethiopia and Uganda respectively.

A model of temporal mass variations within the Earth system developed using GRACE and GNSS data

A model of temporal mass variations within the Earth system were developed using GRACE and GNSS data (Godah et al., 2019b). Time series of monthly vertical deformation of the Earth’s surface for the period between 2008 and 2013 were determined at all 25 ASG-EUPOS stations located in south-eastern Poland. They were obtained by averaging daily vertical coordinates calculated using GAMIT/GLOBK software v.10.7 and the double differencing processing strategy. Monthly vertical deformations were converted into temporal mass variations represented by ΔEWT using Green’s function and Terzaghi’s principle methods. Moreover, monthly ΔEWT for the mentioned period were determined at ASG-EUPOS sites investigated using RL06 GRACE-based GGMs developed by the CSR (Centre for Space Research, University of Texas) computing centre and the NASA’s JPL (Jet Propulsion Laboratory) Mascons solutions.

By combining ΔEWT obtained from GNSS data and the corresponding ones based on GRACE satellite mission data the so called combined models of temporal variations of equivalent water thickness ΔEWT were developed at 25 ASG-EUPOS sites as follows:

$$\Delta EWT_{\text{model}} = \frac{w_1 \cdot \Delta EWT_{\text{GNSS}} + w_2 \cdot \Delta EWT_{\text{GRACE}}}{w_1 + w_2} \quad (1)$$

where w_1 (estimated to 1) and w_2 (estimated to 2) denote the weight for ΔEWT obtained from the GNSS and GRACE satellite mission data, respectively. The estimation of w_1 and w_2 was based on the fit of ΔEWT obtained from the GNSS and GRACE satellite mission data to the corresponding ones obtained from the WaterGAP Global Hydrology Model (WGHM).

Models of ΔEWT developed were evaluated using ΔEWT from WGHM. The main findings reveal that:

- GNSS data can provide valuable information for the determination of ΔEWT . The differences between ΔEWT obtained from the inversion of GNSS-based vertical deformations using the Green's function and the Terzaghi's principle methods are merely negligible.
- GGMs seem more suitable than mascon solutions for the determination of ΔEWT over the area investigated.
- The combination of ΔEWT obtained from GNSS data and GRACE satellite mission data fits better to ΔEWT obtained from WGHM than ΔEWT obtained from GRACE satellite mission data only (Table 3).

Table 3. Improvement of $\Delta EWT_{\text{model}}$ with respect to $\Delta EWT_{\text{GRACE}}$ at locations of ASG-EUPOS sites investigated

GRACE data products	Corr. coeff.		Std. dev. of differences	
	GGMs	Mascons	GGMs	Mascons
Improvement value	0.16	0.26	1.2 cm	1.5 cm
% of stations with improved ΔEWT	80	72	76	60

The groundwater storage (GWS) variations of the main Polish river basins (Vistula and Odra) were independently of previous research of the team of IGiK assessed using GRACE observations, in-situ groundwater level data, GLDAS (Global Land Data Assimilation System) hydrological models, and CMIP5 (the World Climate Research Programme’s Coupled Model Intercomparison Project Phase 5) climate data (Sliwinska et al. 2019a). The GWS was computed by subtracting soil water and snow water (from GLDAS and CMIP5) from the GRACE TWS. The resulting GWS values were evaluated by comparison with in-situ well measurements (Fig. 42). The study revealed that when comparing TWS values, better consistency with GRACE data was obtained for GLDAS than for CMIP5 models. However, the GWS analysis showed better agreement of climate models with the well results.

Rzepecka and Birylo (2020) analysed changes in groundwater level in Poland obtained from direct measurements in wells and groundwater storage anomalies calculated using GRACE observations. The correlations between the thickness of the unsaturated zone at the location of the localization of the wells and the depth of the wells were discussed.

Figure 43 shows a small correlation between the thickness of the unsaturated zone and GWS as well as between the thickness of the unsaturated zone and GRACE. The correlations of GRACE versus the thickness of the unsaturated zone were much larger than the correlations of GWS versus the thickness of the unsaturated zone.

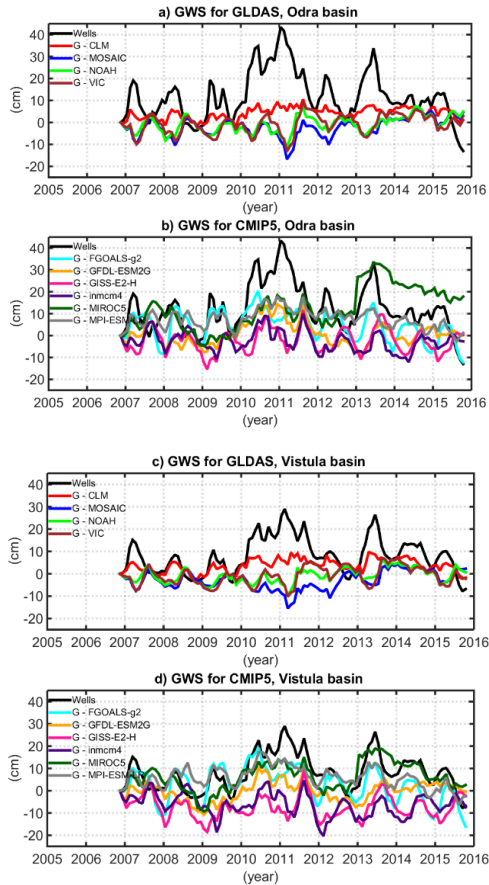


Fig. 42. Comparison of the time series of GWS derived from wells with GWS series obtained from GRACE–GLDAS (a, c) and GRACE–CMIP5 (b, d). Odra (a, b) and Vistula (c, d) basins are considered

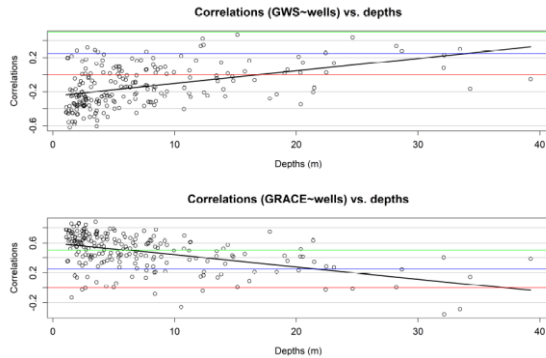


Fig. 43. Correlations between GWS and the thickness of the unsaturated zone (a) and between GRACE and the thickness of the unsaturated zone (b)

The results obtained indicate that GRACE data alone, not reduced by using any model, can best reflect the behaviour of the water level in the wells when they are properly shifted. The changes in water levels in the wells were much greater than the changes in TWS from GRACE or GWS from GRACE and GLDAS. This is probably due to the mean soil porosity.

A geophysical interpretation of polar motion based on the GRACE data and hydrological models

were continued to be investigated by the team of the Space Research Centre (SRC) of the Polish Academy of Sciences (PAS) (Nastula et al., 2019; Nastula and Sliwinska 2020; Sliwinska et al. 2020a). The Hydrological Angular Momentum (HAM) was evaluated by comparison with the residuals of observed polar motion excitation (geodetic residuals, GAO). The level of agreement between HAM and GAO depended on the frequency band considered and was highest for interannual changes (Fig. 44).

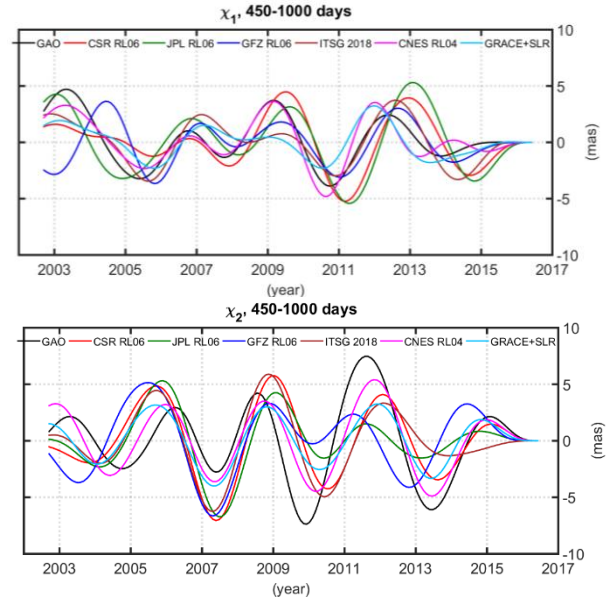


Fig. 44. χ_1 and χ_2 components of GAO and HAM obtained from different GRACE gravity models (CSR RL06, JPL RL06, GFZ RL06, ITSG 2018, CNES RL04) and from the combination of GRACE and SLR (GRACE+SLR). Oscillations with periods of 450–1000 days are considered

The usefulness of gravity models based on kinematic orbits of low-Earth-orbit (LEO) satellites in the study of polar motion excitation was investigated in Sliwinska and Nastula (2019). A number of monthly solutions obtained from GRACE, Swarm, TerraSAR-X, TanDEM-X, MetOp-A, MetOp-B and Jason 2 orbits were validated using GAO. The findings indicated a large impact of orbital altitude and inclination on the accuracy of derived HAM. The orbit parameters excluded MetOp-A, MetOp-B and Jason 2 from further analyses as they provided noisier solutions than other satellites. Seasonal and non-seasonal χ_1 and χ_2 components of GAO and HAM obtained are shown in Figures 45 and 46, respectively. The study showed that HAM series obtained from GRACE and Swarm data were found to be the most consistent with GAO.

Sliwinska et al. (2020b) evaluated the first estimates of HAM/CAM obtained from the GRACE-FO mission. Three different GRACE/GRACE-FO data types were used, namely

ΔC_{21} and ΔS_{21} coefficients, gridded TWS anomalies derived from coefficients of geopotential, and TWS anomalies obtained from mascon solutions (Fig. 47).

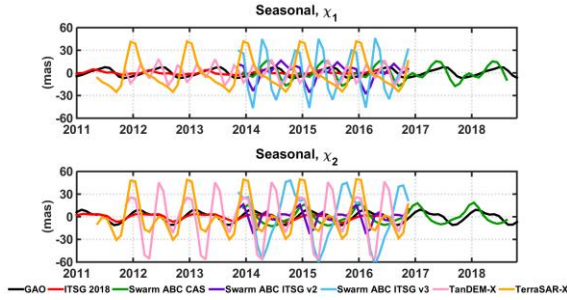


Fig. 45. χ_1 and χ_2 seasonal components of GAO and HAM obtained from ITSG 2018 GRACE solution and solutions based on kinematic orbits of Swarm ABC, TanDEM-X and TerraSAR-X satellites

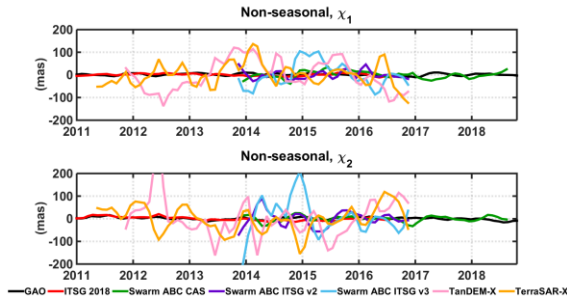


Fig. 46. χ_1 and χ_2 non-seasonal components of GAO and HAM obtained from ITSG 2018 GRACE solution and solutions based on kinematic orbits of Swarm ABC, TanDEM-X and TerraSAR-X satellites

Different methods of HAM/CAM estimation were compared and the compatibility between data from various GRACE/GRACE-FO data centres was investigated. Analysis of data from the first two years of GRACE-FO showed that the consistency between GRACE-FO-based HAM/CAM and GAO is similar to the consistency obtained for the initial period of the GRACE mission, worse than the consistency received for the best GRACE period, and higher than the consistency obtained for the terminal phase of the GRACE mission.

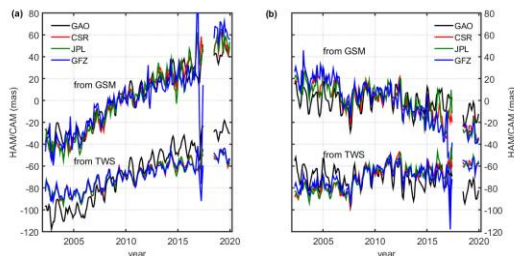


Fig. 47. Time series of χ_1 (a) and χ_2 (b) components of HAM/CAM computed from the GRACE and GRACE-FO monthly solutions provided by various data centres. HAM/CAM are computed from GSM and TWS data. Time series for GAO are added for comparison

The use of national CORS networks for determining temporal mass variations within the Earth's system and for improving GRACE/GRACE-FO solutions

The usefulness of GNSS CORS (Continuously Operating Reference Stations) networks, in particular, the ASG-EUPOS network, for the determination of temporal mass variations within the Earth's system and for improving GRACE/GRACE-FO solutions was investigated (Godah et al., 2020a). Time series of monthly variations of equivalent water thickness $\Delta EWT_{m-GRACE}$ and vertical deformations of the Earth's surface $\Delta h_{m-GRACE}$ for the period 2008-2018 were determined at the 96 sites of the ASG-EUPOS CORS network using RL06 CSR GRACE/GRACE-FO-based GGMs and GNSS data. Moreover, for the same period and GNSS sites, monthly vertical deformations of the Earth surface Δh_{m-GNSS} were determined from GNSS data processed with the use of the GAMIT/GLOBK software v.10.7 and the double differencing processing strategy. Thereafter, ΔEWT_{m-GNSS} were estimated by inverting Δh_{m-GNSS} into water mass variations using Green's function method. Furthermore, combined solutions $\Delta EWT_{m-CombSol}$ were developed by combining ΔEWT_{m-GNSS} with the corresponding ones $\Delta EWT_{m-GRACE}$. Monthly variations of equivalent water thickness determined from GRACE satellite mission data, GNSS data, and combined solutions were compared with the corresponding ones obtained from the WGHM (Water Global Assessment and Prognosis (WaterGAP) Global Hydrology Model). A clear seasonal pattern of $h_{m-GRACE}$ and Δh_{m-GNSS} over the area investigated was shown. Linear trends of these Δh_{m-GNSS} and $\Delta h_{m-GRACE}$ are not fully consistent. Statistics of peak-to-peak variations of the seasonal pattern of the monthly vertical deformations and linear trends of Δh_{m-GNSS} and $\Delta h_{m-GRACE}$ are given in Table 4.

Table 4. Statistics of peak-to-peak variations and linear trends of Δh_{m-GNSS} and $\Delta h_{m-GRACE}$

statistics/trend	Δh_{m-GNSS}	$\Delta h_{m-GRACE}$
Median	21.7 mm	20.0 mm
Min ÷ Max	10.2 ÷ 38.2 mm	13.8 ÷ 21.4 mm
Std.	± 4 mm	± 1.6 mm
Linear trend	1.47 ÷ 2.16 mm/yr	0.67 ÷ 1.86 mm/yr

The combination of monthly ΔEWT from GNSS data of the ASG-EUPOS CORS network with the corresponding ones determined from GRACE satellite mission data improves the determination of ΔEWT . Table 5 provides the percentages of ASG-EUPOS CORS network sites with strong, moderate/weak and no correlations between monthly ΔEWT determined from GRACE satellite mission data ($\Delta EWT_{m-GRACE}$), GNSS data from

ASG-EUPOS CORS network (ΔEWT_{m-GNSS}) and their combined solutions ($\Delta EWT_{m-CombSol}$) with respect to ΔEWT_{m-WGHM} obtained from WGHM. It also gives the values of standard deviation of the differences between each of ΔEWT_{m-GNSS} , $\Delta EWT_{m-GRACE}$ and $\Delta EWT_{m-CombSol}$ with respect to ΔEWT_{m-WGHM} .

Table 5: Percentage of ASG-EUPOS CORS network sites with strong (S), moderate/weak (M/W) and no correlation (NO) between ΔEWT_{m-GNSS} , $\Delta EWT_{m-GRACE}$, and $\Delta EWT_{m-CombSol}$ with respect ΔEWT_{m-WGHM} .

The values of standard deviations of the differences between ΔEWT_{m-GNSS} , $\Delta EWT_{m-GRACE}$, and $\Delta EWT_{m-CombSol}$ with respect to ΔEWT_{m-WGHM}

ΔEWT time series	% of the ASG-EUPOS network sites with:			Std.
	(S)	(M/W)	(NO)	
ΔEWT_{m-GNSS} and ΔEWT_{m-WGHM}	32	56	12	7 cm
$\Delta EWT_{m-GRACE}$ and ΔEWT_{m-WGHM}	57	38	5	5 cm
$\Delta EWT_{m-CombSol}$ and ΔEWT_{m-WGHM}	83	16	1	4 cm

Assessment of orthometric/normal heights changes using GRACE satellite mission data

Temporal variations of orthometric/normal heights $\Delta H/\Delta H^*$ for 24 large river basins over the world (Godah et al., 2020) and over the area of Turkey (Öztürk et al., 2020) were determined using GRACE-based GGMs. Additionally, $\Delta H/\Delta H^*$ over Turkey were also determined using the Green's function method and the Terzaghi's principle approaches. The $\Delta H/\Delta H^*$ determined over Turkey were analysed using the seasonal decomposition (SD) and the Principal Component Analysis/Empirical Orthogonal Function (PCA/EOF) methods, while only the PCA/EOF method was implemented to analyse $\Delta H/\Delta H^*$ for the large river basins. It has been shown that $\Delta H/\Delta H^*$ for the same subarea at different epochs reaches 8 cm over the river basin characterized with strong hydrological signal (i.e. the Amazon basin), while only ca. 2 cm for the river basin of weak hydrological signal (i.e. the Orange basin) and 2.5 cm over Turkey. For 88% of river basins subareas $\Delta H/\Delta H^*$ are correlated with ΔEWT , while no correlations between $\Delta H/\Delta H^*$ and ΔEWT were obtained at river basins subareas located in regions of a very weak hydrological signal (e.g. southern Sahara). For Amazon and Orange basins, the 1st and 2nd PCs (principle components) time series reflect together 95% and 94% of a total variance of $\Delta H/\Delta H^*$ signal, respectively. They exhibited that $\Delta H/\Delta H^*$ over these large river basins are not an artefact, but are a consequence of the processes inducing hydrological mass transport. Over the area of Turkey, models of $\Delta H/\Delta H^*$ developed using the SD method are obviously better than the corresponding models developed using the

PCA/EOF method. The models from the SD method fit quite well, i.e. 95.7–97.0% in terms of correlations. The standard deviations of differences between $\Delta H/\Delta H^*$ data and the corresponding models developed using the SD method range from 0.9 to 1.2 mm. Finally, the Green's function method was found more suitable than the Terzaghi's principle approach for the determination of $\Delta H/\Delta H^*$ over the area of Turkey.

Analysis of the Earth's surface deformations in North-East India and Nepal Himalaya

Seasonal horizontal deformations of the Earth's surface were investigated over North-East India and Nepal Himalaya using GPS and GRACE satellite mission data (Ray et al., 2021). The correlation coefficient value between time series of horizontal seasonal deformations of the Earth's surface in the north component obtained from GPS and GRACE satellite mission data has positive value at nearly 89% of GPS stations. Median values of the correlation coefficients in the north and east components are 0.61 and 0.2, respectively. They also revealed a positive reduction of Weighted Root Mean Square (WRMS), in the case of north component, at ~83% of GPS stations in comparison to the 58% in the case of the east component. Median value of Nash-Sutcliffe model Efficiency (NSE) values in the north and east components is 0.28 and -0.01, respectively.

9. Monitoring gravity changes

Monitoring gravity changes at the Borowa Gora Observatory with the iGrav-027 superconducting gravimeter was continued in 2019 and 2020. In 2019 a nearly 1080 day time series (Fig. 48) was analysed (Dykowski et al., 2019b). The analysis included scale factor determination with the use of LaCoste&Romberg gravimeters as well as drift function evaluation. The drift was evaluated using monthly side by side surveys with the A10-020 gravimeter which allowed to evaluate the long term drift of the iGrav-027 gravimeter is within single $\mu\text{Gal}/\text{year}$.

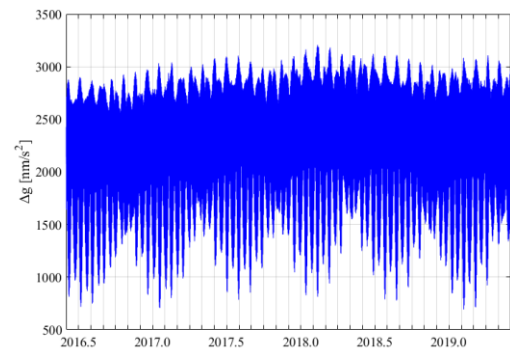


Fig. 48. Tidal record with the iGrav-027 gravimeter from first 1080 days of operation

Furthermore, the analysis included tidal adjustment with the use of the updated Eterna 3.40 software, the ET34-X-V73 (Schueller, 2015), in order to eliminate the tidal signal for further analysis. Tidal adjustment resulted in the standard error of 0.413 nm/s^2 with residuals mostly within $\pm 1 \text{ nm/s}^2$ (Fig. 49).

Drift and adjusted tide corrected residuals (Fig. 50 – black) were further corrected for the MERRA2 non local atmospheric loading effect (from EOST Loading Service) and compared with MERRA2 (Fig. 50 – red) and GLDAS2 (Fig. 50 – green) hydrological loading models (also from EOST Loading Service) (Fig. 50).

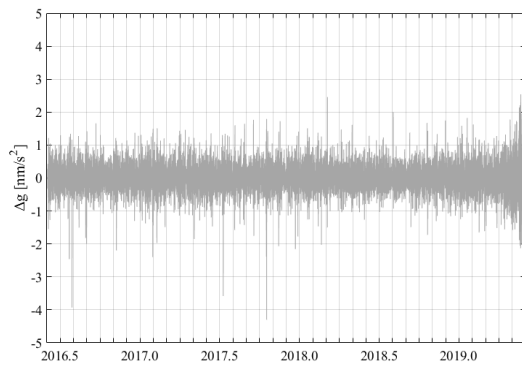


Fig. 49. Tidal adjustment residuals from the iGrav-027 gravimeter

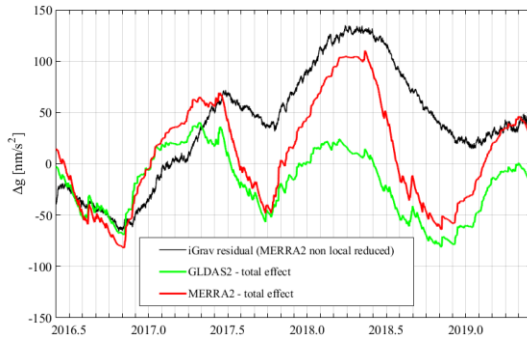


Fig. 50. Comparison of the iGrav-027 gravimeter residuals and MERRA2 and GLDAS2 hydrological loading models

The realization of EPOS-PL and EPOS-PL+ projects resulted in significant improvement in coverage of Poland with stations recording gravity changes. In late 2018 two gPhoneX gravimeters were installed by the Central Mining Institute in the Upper Silesian Region (Mutke et al., 2019; Dykowski et al., 2019d; Kotyrba and Kortas, 2020). Then, in 2019 another gPhoneX unit was installed at the WUELS. In 2020 the Space Research Centre installed the gPhoneX gravimeter at Borowiec Astro-Geodynamical Observatory. Outside EPOS-PL and EPOS-PL+ projects the Polish Geological Institute installed the gPhoneX gravimeter at Holowno facility. Figure 51 presents all the current tidal gravimeters recognized in Poland within the

framework of the EPOS-PL project. All the gravimeters marked green in Figure 51 currently provide data to the Gravimetric Observations Research Infrastructure Centre at IGIK operating within the EPOS-PL project.

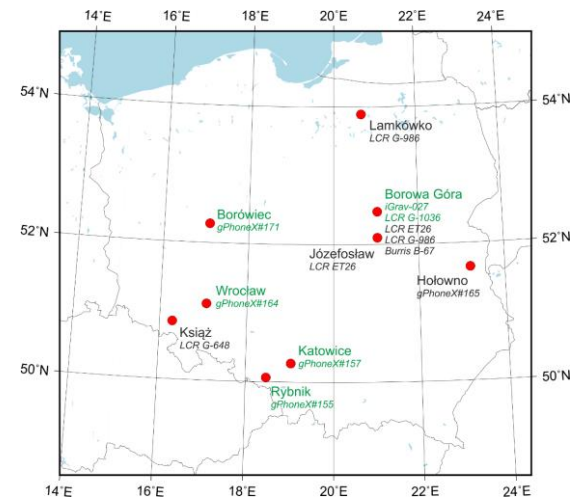


Fig. 51. Gravimetric tidal records in Poland as recognized in late 2020 within the EPOS-PL project

10. Activities in Satellite Laser Ranging and their use

In 2019 and 2020 the Satellite Laser Ranging Station Borowiec (BORL) of the SRC of PAS tracked 100 different objects, satellites and space debris (cooperative and uncooperative targets). The total number of recorded passes in 2019 is 1468 (Fig. 52). 44 objects tracked were satellites: 30 were Low Earth Orbit (LEO) and 14 were Medium Earth Orbit (MEO) objects. The average RMS ranged from 1.20 cm to 3.81 cm (1079 passes and 15197 normal points). The other 38 objects were typical space debris, inactive (defunct) satellites and rocket bodies from the LEO regime. The average RMS ranged from 2.04 cm to 221.72 cm (388 passes and 4074 normal points).

The COVID-19 pandemic made 2020 a very difficult and very challenging year. However, it was a good year for the laser ranging station BORL7811, which successfully tracked 97 objects, with a total of 2050 full passes (Fig. 53). Forty of these objects were satellites: 27 LEO; and 13 MEO for a total of 1352 passes, 18644 normal points, and pass RMS ranging from 1.49 cm to 4.11 cm. Fifty-seven objects were typical space debris, such as inactive (defunct) satellites and rocket bodies (boosters) from the LEO regime giving 698 passes, 7396 normal points and pass RMS ranging from 1.42 cm to 187.58 cm. These targets were observed within the framework of the Space Debris Study Group run by the International Laser Ranging Service (ILRS) and internal contracts signed with European Space Agency (ESA) and European Consortium EUSST (<https://www.eusst.eu/>).

The information about the position and behaviour of space debris such as defunct satellites is very important from the point of view of future debris removal missions (e.g. ENVISAT). The number of space junk is increasing rapidly. Currently there are more than 20 000 orbiting objects with diameter ≥ 10 cm (Fig. 54).

Not only positions of all these objects are needed but also a precise information about their rotation/tumbling and orientation in space. Laser measurements recorded by the BORL station support global research on the determination of space debris spin dynamics (ENVISAT, ERS-1, ERS-2, OICETS, Seasat-1, TOPEX/Poseidon and others), which is essential to improve theories of the motion of artificial satellites, including space debris. All results were sent to the Crustal Dynamics Data Information System (CDDIS), Eurolas Data Center (EDC) and Space Debris databank in Graz, Austria.

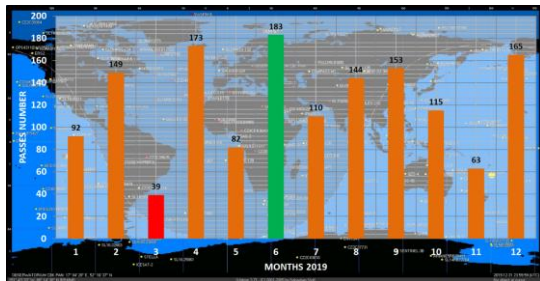


Fig. 52. Number of passes recorded by the BORL station (active satellites and debris) in 2019 (green column – the highest number of passes; red column – the lowest number of passes)

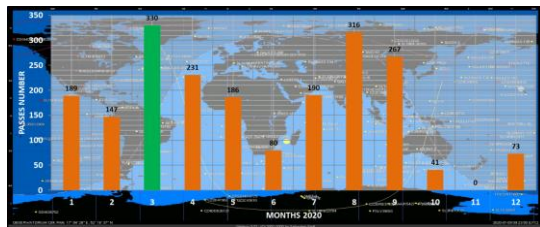


Fig. 53. Number of passes recorded by the BORL station (active satellites and debris) in 2020 (green column – the highest number of passes)

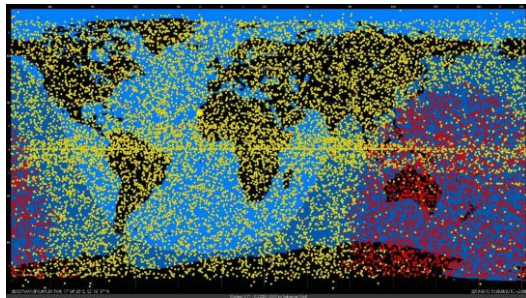


Fig. 54. Orbiting objects with diameter ≥ 10 cm (Orbitron software¹⁹)

12 of satellites tracked in 2019 in the framework of ILRS were geodetic-geodynamic satellites (Ajisai, Etalon-1, Etalon-2, Geo-1K-2, GRACE-FO-1, GRACE-FO-2, LAGEOS-1, LAGEOS-2, LARES, LARETS, STARLETTE and Stella) which gave in total 443 passes and 4933 normal points. Details concerning observations of these satellites in 2019 are presented statistics in Table 6.

The largest number of passes (100), of returns (125946), and of normal points (923) was obtained for LAGEOS-1. The mean RMS ranges from 1.55 cm for LAGEOS-1 3.81 cm for Ajisai.

Similar statistics for year 2020 of a total of 552 passes and 5745 normal points is presented in Table 7. The highest number of passes (111), returns (189595) and normal points (1387) were obtained for AJISAI. Mean RMS ranged from 1.51 cm (for LARES) to 3.61 cm (for ETALON-2).

Table 6. Details concerning observations of geodetic satellites in 2019

Sat. name	Passes	Returns	Normal points	Avg RMS [cm]
Ajisai	62	84860	785	3.81
Etalon-1	3	453	14	3.76
Etalon-2	4	295	20	2.60
Geo-1K-2	3	4229	31	2.19
GRACE-FO-1	23	9880	564	3.08
GRACE-FO-2	11	5291	285	2.88
LAGEOS-1	100	125946	923	1.76
LAGEOS-2	43	43780	440	1.82
LARES	75	37186	821	1.55
LARETS	56	21245	405	2.16
STARLETTE	53	46889	573	2.31
Stella	13	7851	103	2.07

Table 7. Details concerning observations of geodetic satellites in 2020

Sat. name	Passes	Returns	Normal points	Avg RMS [cm]
Ajisai	111	189595	1387	3.41
Etalon-1	0	0	0	0
Etalon-2	3	364	14	3.61
Geo-1K-2	6	4705	38	2.22
GRACE-FO-1	21	10077	432	3.45
GRACE-FO-2	15	7731	350	3.19
LAGEOS-1	46	45220	423	1.73
LAGEOS-2	50	30870	388	1.78
LARES	104	36486	1004	1.51
LARETS	92	37412	713	1.98
STARLETTE	97	70903	931	2.02
Stella	7	5109	65	2.02

The quality of the BORL laser sensor is regularly evaluated based on the tracking results of LAGEOS-1 and LAGEOS-2 satellites in the form of station performance report. Figures 55 and 56 shows a significant improvement of both quality and effectiveness of the measurements of the BORL station as compared to the previous years of its activity. The average LAGEOS RMS is on the level 17–18 mm (Fig. 55), the average LAGEOS measurements in a normal point is approx. 150

¹⁹ <http://www.stoff.pl/>

(Fig. 56) and the average LAGEOS fullrate measurements per pass is approx. 1800 (Fig. 57).

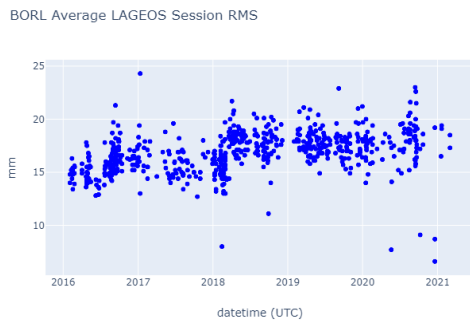


Fig. 55. LAGEOS normal point RMS from last 5 years for BORL station²⁰

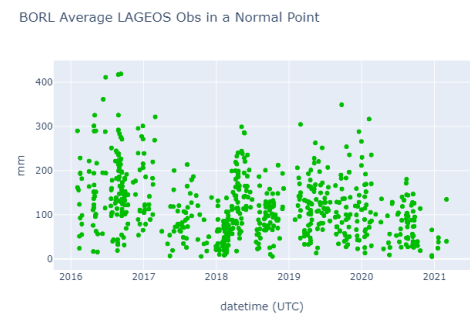


Fig. 56. LAGEOS measurements in a normal point from last 5 years for BORL station²¹

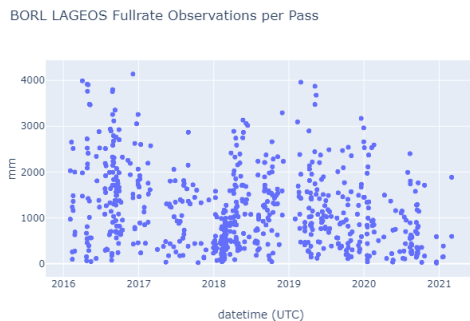


Fig. 57. LAGEOS full rate measurements per pass from last 5 years for BORL station²²

In years 2019–2020, the team of Borowiec Observatory worked on a new software dedicated for the reduction of the laser measurements (Figs. 58, 59, 60).

This software is adopted to the newest operating systems (Windows/Linux), with very flexible graphic interface and allows for determination of

²⁰ https://ilrs.gsfc.nasa.gov/network/stations/active/perfPlots/BORL_Lageos_NPT_RMS.html

²¹ https://ilrs.gsfc.nasa.gov/network/stations/active/perfPlots/BORL_Lageos_NPT_OBS.html

²² https://ilrs.gsfc.nasa.gov/network/stations/active/perfPlots/BORL_Lageos_FR_OBS.html

different parameters, i.e. residuals O–C, normal points, RMS of normal points, RMS of observation, time bias, range bias. The code of the software has been created based on the specifications and requirements given by ILRS²³. At present the software is in testing phase.

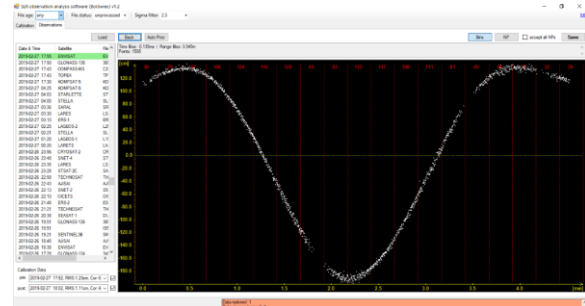


Fig. 58. Results of the measurements reduction of ENIVSAT (O–C residuals)

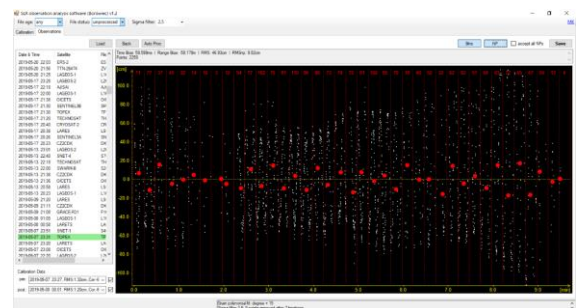


Fig. 59. Results of the measurements reduction of TOPEX/Poseidon (O–C residuals and normal points)

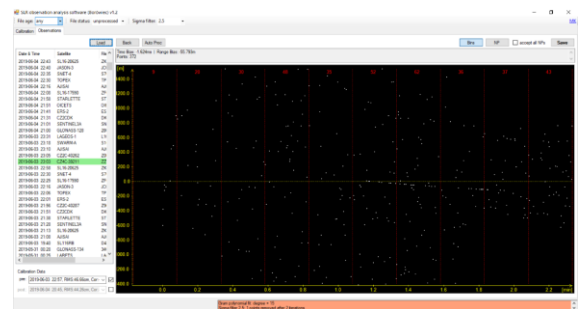


Fig. 60. Results of the measurements reduction of Chang Zheng 4C rocket (O–C residuals with noise points)

The new big task in the activity of the BORL station are orbital calculations of space debris based on laser measurements. This topic is still under development.

In 2019, the orbital calculations of 13 space debris objects were performed (Russian and Chinese boosters from LEO regime). The aim of this analysis was to show how the laser measurements from one station improve orbits of the tracked rockets. Calculations were performed

²³ https://ilrs.cddis.eosdis.nasa.gov/data_and_products/data/npt/npt_algorithm.html

using the advanced orbital programme GEODYN-II, basing on laser measurements of BORL station. The results of comparison of input ephemerides vs. positions obtained from laser measurements are presented in Figure 61.

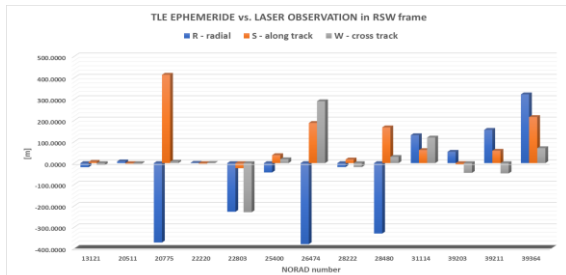


Fig. 61. Input TLE ephemerides vs. laser measurements in RSW frame

For all analysed targets the differences between the used TLE (initial orbital elements) and performed observations of BORL station (corrected elements/positions) are given in RSW frame (radial, along-track, cross-track). In conclusion, the one short observation from a dozen to several dozen seconds of analysed objects improves the variance-covariance matrix by 20–40% (Lejba et al., 2020).

In the years 2019–2020 the BORL station focused on the SST programme, which constitutes one of the pillars of the Space Situational Awareness (SSA) programme implemented by the ESA (Space Safety in the next years) and the EC (EUSST Consortium) (Konacki et al., 2019). The SST programme is dedicated to monitoring (observation, detection, identification) of active and inactive satellites, discarded launch stages and fragmentation debris orbiting Earth. The BORL station is responsible for research and development in SLR. Poland is an official member of the EUSST Consortium, and the SRC PAS is one of the members of the Polish SST consortium.

The BORL station operates a second independent optical-laser system, dedicated to the SST programme (Krynski and Rogowski, 2019; Suchodolski, 2019).

One of the most important scientific achievements in 2020 of the BORL station team was the computation of the coordinates of the BORL station based on LAGEOS measurements performed by the ILRS network for the years 2016–2019. The results obtained confirm the high quality of the BORL station’s data.

The local Love and Shida numbers (parameters h_2 and l_2) for the Australian Yarragadee and Mount Stromlo SLR stations were analysed based on data from the Stella, STARLETTE, LAGEOS-1 and LAGEOS-2 satellites for the period 1 January 2014 to 1 January 2019 (Jagoda et al., 2020). Quality of SLR station coordinates determined from laser ranging to the LARES satellite was also analysed by comparing the results with the respective ones

obtained from the LAGEOS satellites (Schillak et al., 2021).

ILRS Associated Analysis Center for MGEX

The Wrocław University of Environmental and Life Sciences (WUELS) hosts the Associated Analysis Center of the ILRS (Otsubo et al., 2019; Pearlman et al., 2019). The Center provides products for validating orbits of Galileo, GLONASS, BeiDou, and QZSS satellites generated by the Center for Orbit Determination in Europe with respect to laser observations collected by SLR stations distributed worldwide, and information about satellites of new GNSS systems and the characteristics of laser stations. The Center generates daily reports with the features of the quality of the orbits of GNSS satellites and the quality of laser observations provided by stations and enables performing online analyses and data visualization. The high quality of GNSS orbits is important for the high-quality positioning and navigation based on new GNSS systems (Hadas et al., 2019; Katsigianni et al., 2019) as well as for the realization of the geodetic reference frames and the determination of global geodetic parameters (Zajdel et al., 2019a, 2019b, 2020). The service is available through a dedicated website²⁴.

11. Geodynamics

IGiK, WAT and WUELS, integrated into the GGOS-PL network, together with the Institute of Geophysics of the Polish Academy of Sciences and with some other institutions continued a common geodynamics research in the framework of the EPOS-PL project – the Polish Earth science infrastructure integrated with the European Plate Observing System Programme (EPOS) programme.

Activities on developing centres of research infrastructure for geomagnetic and gravimetric data integrated with GNSS infrastructure are continued (Krynski et al., 2019c; Werner et al., 2019).

A three-year the program of semi-annual absolute gravity measurements with the FG5-230 gravimeter of WUT at two stations of the geodynamics monitoring network MoGe-PL of the Polish Geological Institute was started in 2019 (Krynski et al., 2019b).

Absolute gravity surveys with the A10-020 gravimeter on MUSE polygons were continued within EPOS-PL project (Mutke et al., 2019, Dykowski et al., 2019d) in 2019 and 2020. All together seven repeated campaigns were performed in total on 11 stations used for reference for densification survey with relative instrument on further 200 stations. Absolute stations (marked red) and half of the relative stations (marked black) are presented in Figure 62.

²⁴ www.govus.pl

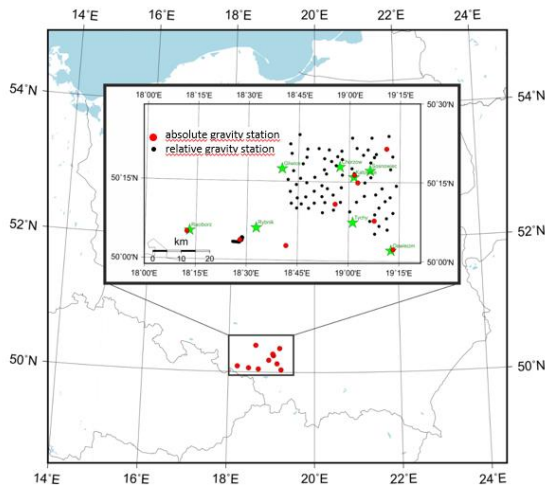


Fig. 62. Gravity control at MUSE polygons for repeated A10-020 surveys

Comparison of vertical deformations of the Earth's surface obtained using GRACE-based GGMs and GNSS data for the south-eastern Poland

The vertical deformations of the Earth's surface induced by temporal mass loading, e.g. hydrological loading, at 25 ASG-EUPOS sites in south-eastern Poland were investigated. The comparison of these vertical deformations of the Earth's surface obtained using RL06 GRACE-based GGMs and GNSS data covering the period between 2008 and 2013 was conducted. GNSS data and GRACE-based GGMs were processed with the GAMIT/GLOBK and the IGiK-TVGMF software, respectively. The results obtained indicate that monthly vertical deformations of the Earth's surface determined using GNSS data are generally in a good agreement with the corresponding ones obtained from GRACE satellite mission data. Coefficients of correlation between these vertical deformations range from 0.60 to 0.90 and standard deviations of their differences are in the range of 2.6–5.7 mm (Godah et al., 2019c, 2019d, 2020).

Research conducted at IGiK showed that recordings of tidal gravimeters can be used to provide complementary information on the distribution of velocities of seismic wave in the Earth's interior. Gravimetric recordings of earthquakes in a period range of 20–1000 s correspond to seismic ones very well after application transfer function (Karkowska and Wilde-Piorko, 2019; Wilde-Piorko and Karkowska, 2019). Group dispersion curves of seismic surface waves have been measured up to the periods of 600 s from the recordings of tidal gravimeters and up to the periods of 300 s from the recordings of co-located typical broadband seismometers (Wilde-Piorko and Karkowska, 2019; Karkowska and Wilde-Piorko, 2020). The phase velocities of seismic Rayleigh waves measured between two

tidal gravimeters are similar with ones measured between two co-located broad-band seismometers (Wilde-Piorko and Karkowska, 2020). Moreover, the phase velocities can be determined for much higher periods based on the gravimetric data. Linear inversion of measured dispersion curves allowed for the estimation of seismic structure down to the depth of 1800 km and 800 km, respectively, for gravimeters and seismometers (Wilde-Piorko and Karkowska, 2019; Karkowska and Wilde-Piorko, 2020). Further research on an estimation of seismic structure based on an inversion of group dispersion curves of fundamental mode of seismic Rayleigh waves shows that values of the shear wave velocities in the Earth's mantle obtained from the linear inversion reproduce the velocities of the initial model (Karkowska and Wilde-Piorko, 2020). The observed details are unreliable, because of the low sensitivity of the long period surface waves. And the results of the Monte Carlo inversion of the same data set show that a reliable 1-D model of Earth's mantle can be determined down to a depth of 1800 km and consists of several homogeneous layers.

The GNSS data recorded with sampling rate of 10-100 Hz and observations processed in kinematic mode provide high-rate position series enabling the determination of high-frequency time displacements. Such time series can be applied for seismic monitoring, earthquake and tsunami early warning systems, infrastructure monitoring, i.e. bridges and high buildings. The motion of GNSS permanent stations during three natural earthquakes in Italy and Nepal of magnitudes over 6.1 were investigated with the use of Precise Point Positioning (PPP) technique and the data obtained by seismic sensors (Kudlacik et al., 2019). It has been shown that the sensitivity of GPS PPP kinematic high-rate positioning with position domain filtering using a band-pass Butterworth filter on small samples of position time series is sufficient to obtain dynamic co-seismic displacements in good agreement with SM data and provides reliable waveforms (Fig. 63). The average correlation coefficient between GPS and SM displacements after filtering increased from 0.54 to 0.75. The amplitudes of dynamic deformations increased from a few millimetres to meters. This demonstrates that PPP position estimates fluctuation (sidereal effect) and noise can be successfully reduced by the band-pass filtering. In connection with analysis using EPOS-PL infrastructure, this approach was applied to study the mining-induced earthquake in Poland on 29 January 2019. The results of comparison GNSS with seismological data from co-located stations are satisfactory, with correlation coefficients up to 0.94 (Fig. 64).

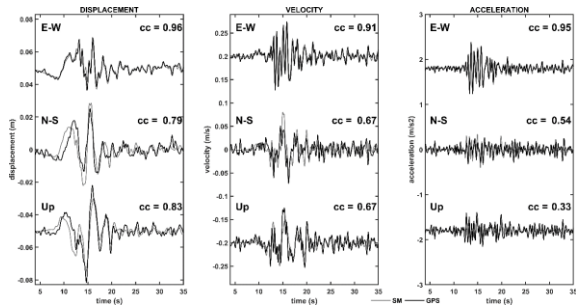


Fig. 63. GPS (black) and SM (grey) displacement, velocity and acceleration time series of Norcia earthquake (2016-10-30 06:40:18 UTC, Mw 6.6) cropped to analysed time with correlation coefficients of station GUMA. GPS data is band-pass filtered on cut-off frequencies of 0.05–2.00 Hz; SM data is band-pass filtered by the Istituto Nazionale di Geofisica e Vulcanologia (Luzi et al., 2016) on cut-off frequencies of 0.05-70.00 Hz and then low-pass filtered on a cut-off frequency of 2 Hz

More than 18 000 GNSS permanent stations all over the world provide coordinate time series that provide useful information concerning local and global geodynamics. The influence of geophysical signals (non-tidal atmospheric loading – NTAL, non-tidal ocean loading – NTOL, hydrology – HYDL; local geodynamic signals and others) on coordinate variations was investigated (Kaczmarek, 2019). The distribution of spatial deformation distribution from geophysical models (NTAL, NTOL, HYDL) was analysed. Figure 64 shows distribution of spatial correlation coefficients for the sum (SUM=NTAL+NTOL+HYDL) of geophysical deformations.

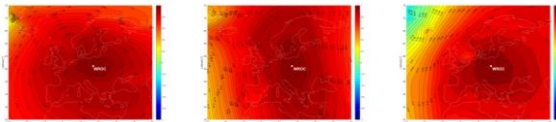


Fig. 64. Spatial distribution of correlation coefficients for SUM geophysical deformation

The range of deformation is regional for all analysed GNSS stations (black dots) (Fig. 65).

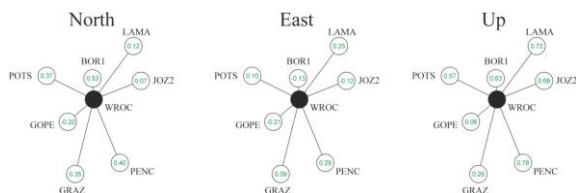


Fig. 65. Spatial distribution of correlation coefficients between coordinates of the WROC station and coordinates of the neighbouring GNSS stations

The greatest effect on coordinates variation should have geophysical deformations and they should be of the same value for all analysed stations but is not the case. In addition, correlation coefficients between coordinate time series

calculated (Fig. 65) confirmed that the stations investigated register different periodic signals, despite regional range of geophysical deformation. Probably it is caused by other, non-identified signals which occur only locally.

Bogusz et al. (2019) proposed an optimum strategy for GPS position time series analysis to study the Post-Glacial Rebound effect. They proved that the proper treatment of either deterministic or stochastic components of the time series is indispensable to obtain reliable vertical velocities along with their uncertainties. They tested their approach on Scandinavia, where the maximum values of uplift may reach even 11.0 mm/yr. The comparison of the present-day motion predicted by the newest Glacial Isostatic Adjustment (GIA) ICE-6G_C (VM5a) and previous ICE-5G models showed good correlation with GPS-derived Vertical Land Motion (VLM), except regions with significant present-day ice melting (Fig. 66).

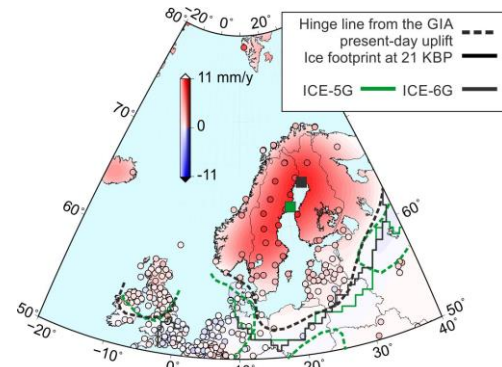


Fig. 66. The vertical rates derived from the GPS position time series

Klos et al. (2019) reassessed the absolute and relative sea level changes at 38 tide gauge stations in the earthquake-affected Western North Pacific for the 1993-2015 period, focusing on the Vertical Land Motion. They introduced a new methodology of non-linear motion presentation using GPS position time series by accounting for co-seismic offsets, changes in the vertical velocities, and post-seismic relaxation. They showed that introducing a new non-linear VLM model improves absolute tide gauge sea level estimates by 20% on average. Finally, they demonstrated that for the reconstructed Western North Pacific sea level, altimetry agrees best with tide gauge data corrected employing the new non-linear VLM model. By continuation of this research, Fenoglio et al. (2020) analysed various standard and improved SAR altimetric products to study their impacts on the estimation of the coastal sea level variability in the last 10 km. They showed that the difference of the trends of altimetry and tide gauge (AL-TG) co-located time series agrees with the GPS rates within 1.5 mm/yr at half of the co-located locations, with AL-TG error larger than the

error of the GPS rate by a factor bigger than two. Klos et al. (2020) investigated the sub-seasonal deformations sensed by GPS, usually less well resolved, to obtain unbiased estimates of GPS vertical velocity and its uncertainty. They used GRACE-assimilating land surface model and concluded, that its output removes the effect of high-frequency hydrological deformations, providing less correlated residuals. Lenczuk et al. (2020) focused on the Earth's crust deformations resulting from hydrology mass changes, as observed by GRACE gravity mission and approximated using WGHM (WaterGAP Global Hydrological Model) and GLDAS (Global Land Data Assimilation System) hydrological models. The analysis was performed for the European area, divided into 29 river basins. They found that the eastern part of Europe is characterized by the largest annual amplitudes of hydrology-induced Earth's crust deformations, which decrease with decreasing distance to the Atlantic coast. They showed, that GLDAS largely overestimates annual amplitudes in comparison to GRACE and WGHM, moreover hydrology models underestimate trends, which are observed by GRACE.

Modern vertical crustal movements of the southern Baltic coast from tide gauge, satellite altimetry and GNSS observations were analysed (Kowalczyk et al., 2019). The linear trend estimation was calculated for the tide gauge and SLA time series to analyse velocity. Additionally, at each station, the correlation coefficient between the satellite altimetry and the tide gauge data were computed in all of the analysed locations (Pajak and Kowalczyk, 2019). The mean coefficient of correlation between the corresponding time series with trends removed from satellite altimetry and tide gauges is 0.92. Figure 67 shows the correlations between the satellite altimetry and tide gauge results (1993-2017).

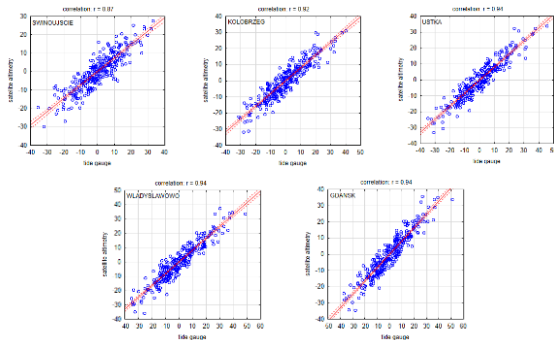


Fig. 67. Correlation coefficients between the satellite altimetry and tide gauge data (blue open circles – plot of the data dispersion and area marked by the dashed red lines – 95% confidence interval of the regression line)

The overall direction of changes in the mean level of the Baltic Sea for Polish tide gauge stations was positive (Kowalczyk, 2019). The data are not

referred to the same reference level, which causes differences between particular values in the same epoch.

The absolute differences in the mean sea level between extreme values for the same time interval (1951–2015) range from 77 mm (Swinoujście) to 114 mm (Gdańsk) (Fig. 68). Vertical lines indicate years in which the values of the mean sea level change the direction, i.e. rise or drop.

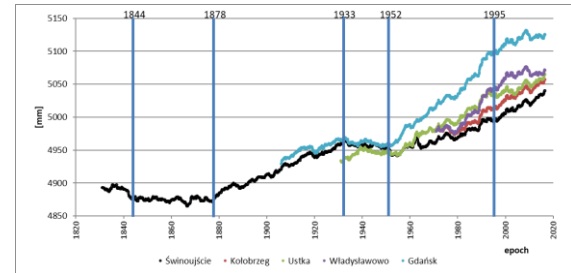


Fig. 68. Moving averages for analysed tide gauge stations

Determination of Earth rotation parameters and geocenter motion using GNSS

The Earth Rotation Parameters (ERPs) are time-variable global geodetic parameters with a purely geophysical origin. ERPs shall be independent of the satellite constellation used in the processing; however, various systematic errors occur in the ERPs derived from GNSS and other space geodetic techniques. Zajdel et al. (2020) and (2021a) highlighted existing differences in the time series of ERPs when using different GNSS constellations. They analysed the daily and sub-daily series of ERPs estimated using GPS, GLONASS, and Galileo observations. The conducted research highlighted that any system-specific ERPs are affected by the orbital and draconitic signals. The GNSS-based products, including ERPs, are sensitive to the modelling issues, including the accuracy of the background models, the approach for handling solar radiation pressure acting on GNSS orbits, or the orbit characteristics, such as satellite revolution periods.

The orbital signals are distinguishable in all system-specific ERPs at the periods that arise from the resonance between the Earth's rotation and the satellite revolution period, e.g. 8.87 h, 34.22 h, 3.4 days for Galileo; 7.66 h, 21.29 h, 3.9 days, 7.9 days for GLONASS; 7.98 h (S3 tidal term), 11.97 h (S2 tidal term), and 23.93 h (S1 tidal term) for GPS. In the Galileo and GLONASS solutions, the artificial non-tidal signals' amplitudes reach up to 30 μ s. The GPS-derived sub-daily ERPs suffer from the overlapping periods of the diurnal and semidiurnal tidal terms and the harmonics of the GPS revolution period. After recovery of 38 sub-daily tidal terms, the Galileo-based model is more consistent with the external models than the GPS-based model, especially in the prograde diurnal band (Zajdel et

al., 2021a). The results confirmed that the Desai–Sibois model of sub-daily ERPs is more consistent with GNSS observations than the currently recommended model in the IERS 2010 Conventions. Moreover, GPS-based length-of-day (LoD) is systematically biased with respect to the IERS-C04-14 values with a mean offset of $-22.4 \mu\text{s/day}$. The Galileo-based and GLONASS-based solutions are almost entirely free of this issue (Zajdel et al., 2020). As opposed to the individual system-specific solutions, the multi-GNSS solution is not affected by most of the system-specific artifacts. Thus, multi-GNSS solutions are clearly beneficial for the estimation of both daily and sub-daily ERPs.

The GNSS orbits must be of superior quality in order to derive high-quality ERPs and geocenter coordinates. Bury et al. (2020) studied the impact of non-gravitational forces acting on Galileo satellites, including the direct solar radiation pressure, albedo, Earth's infrared radiation, antenna thrust, and the B- and Y-biases. Most of the perturbing forces can successfully be accounted for when information about satellite construction and surface properties is available. This is the case for the Galileo system because satellite metadata have been released by the European GNSS Agency (GSA). Bury et al. (2019) employed the Galileo metadata to construct the a priori box-wing model for Galileo satellites. On the top of the a priori model, a small set of empirical parameters must be estimated to account for mismodelled forces and variable external conditions (Bury et al. 2019, 2020).

Zajdel et al. (2021b) employed the model derived by Bury et al. (2020) to derive geocenter coordinates from GPS, GLONASS, and Galileo constellations by testing different sets of additionally estimated empirical orbit parameters. The geocenter coordinates based on the GLONASS satellites turned to be affected by unrealistic spurious signals and strong correlations between orbit parameters and the Z component of geocenter coordinates. Despite that, the Galileo system consists of three nominal orbital planes, thus similarly to GLONASS, the Galileo-based geocenter coordinates are much less affected by orbit modelling issues. Additionally, two Galileo satellites accidentally launched into highly-eccentric orbits, stabilize the Galileo-based geocenter coordinates. Currently, the best possible geocenter coordinates based on GNSS data can be derived using the combination of GPS and Galileo data with the a priori box-wing model (Zajdel et al. 2021b).

Acknowledgements

The following researchers submitted data used to elaborate this report: Andrzej Araszkiewicz, Janusz Bogusz, Pawel Dabrowski, Przemyslaw Dykowski,

Walyeldeen Godah, Jan Krynski, Pawel Lejba, Tomasz Liwosz, Adam Lyszkowicz, Jolanta Nastula, Grzegorz Nykiel, Tomasz Olszak, Jerzy Rogowski, Jaroslaw Somla, Krzysztof Sosnica, Malgorzata Szelachowska, Marek Trojanowicz, Pawel Wielgosz, Monika Wilde-Piorko.

References

- Araszkiewicz A., Podkowa A., Kiliszek D., (2019): *Height variation depending on the source of antenna phase centre corrections: LEIAR25.R3 case study*, Sensors 2019, 19(18), 4010; doi: 10.3390/s19184010
- Araszkiewicz A., Kiliszek D., (2020): *Impact of Using GPS L2 Receiver Antenna Corrections for the Galileo E5a Frequency on Position Estimates*, Sensors 2020, 20, 5536; doi: 10.3390/s20195536
- Arnold D., Montenbruck O., Hackel S., Sosnica K., (2019): *Satellite laser ranging to low Earth orbiters: orbit and network validation*, Journal of Geodesy, Vol. 93, No 11, doi: 10.1007/s00190-018-1140-
- Baldysz Z., Nykiel G., (2019): *Improved Empirical Coefficients for Estimating Water Vapor Weighted Mean Temperature over Europe for GNSS Applications*, Remote Sensing, 11(17), pp. 1–15, doi: 10.3390/rs11171995
- Bogusz J., Klos A., Pokonieczny K., (2019): *Optimal strategy of the GPS position time series analysis for the Post-Glacial Rebound investigation in Europe*, Remote Sensing, 11, 1209, doi: 10.3390/rs11101209
- Bury G., Sosnica K., Zajdel R., (2019a): *Impact of the Atmospheric Non-tidal Pressure Loading on Global Geodetic Parameters Based on Satellite Laser Ranging to GNSS*, IEEE Transactions on Geoscience and Remote Sensing, Vol. 57, No 6, pp. 3574–3590. doi: 10.1109/TGRS.2018.2885845
- Bury G., Sosnica K., Zajdel R., (2019b): *Multi-GNSS orbit determination using satellite laser ranging*, Journal of Geodesy, Vol. 93, No 12, Germany 2019, pp. 2447–2463. doi: 10.1007/s00190-018-1143-1
- Bury G., Zajdel R., Sosnica K., (2019c): *Accounting for perturbing forces acting on Galileo using a box-wing model*, GPS Solutions, 23(3), 74. doi: 10.1007/s10291-019-0860-0
- Bury G., Sosnica K., Zajdel R., Strugarek D., (2020): *Toward the 1-cm Galileo orbits: challenges in modeling of perturbing forces*, Journal of Geodesy, 94(2), 16. doi: 10.1007/s00190-020-01342-2
- Bury G., Sosnica K., Zajdel R., Strugarek D., Hugentobler U., (2021): *Determination of precise Galileo orbits using combined GNSS and SLR observations*, GPS Solutions, Vol. 25, No 11. doi: <https://doi.org/10.1007/s10291-020-01045-3>
- Cellmer S., Nowel K., Fischer A., (2021): *A search step optimization in an ambiguity function-based GNSS precise positioning*, Survey Review, published online: 17 Feb 2021, doi: 10.1080/00396265.2021.1885947
- Czaplewski K., Wisniewski Z., Specht C., Wilk A., Koc W., Karwowski K., Skibicki J., Dabrowski P., Czaplewski B., Specht M., Chrostowski P., Szmaglinski J., Judek S., Grulkowski S., Licow R., (2020): *Application of Least Squares with Conditional Equations Method for Railway Track Inventory Using GNSS Observations*, Sensors 2020, 20(17), 4948, doi: 10.3390/s20174948
- Dabrowski P.S., (2019): *Accuracy of Geopotential Models Used in Smartphone Positioning in the Territory of Poland*, IOP Conf. Series: Earth and Environmental Science 221: 012080. doi: 10.1088/1755-1315/221/1/012080

- Dawidowicz K., (2019): *Sub-hourly precise point positioning accuracy analysis – case study for selected ASG-EUPOS stations*, Survey Review, doi: 10.1080/00396265.2019.1579988
- Dawidowicz K., Rapinski J., Wielgosz P., Smieja M., Kwasniak D., Krzan G., Golaszewski P., Baryla R., Krypiak-Gregorczyk A., Janicka J., Tomaszewski D., Brzostowski K., Grzegory T., Grec F.C. Strataki S., (2019a): *ASTRI/UWM EGNSS receiver antenna calibration facility: current status*, 7th International Colloquium On Scientific and Fundamental Aspects of GNSS, 4–6 September 2019, ETH Zürich, Switzerland.
- Dawidowicz K., Rapinski J., Wielgosz P., Smieja M., Brzostowski K., Gregory T., Grec F.C., (2019b): *System for EGNSS receivers antennas calibration - current status of the project*, International Symposium On Applied Geoinformatics, Yildiz Technical University, 7–9 November 2019, Istanbul, Turkey.
- Drozdzewski M., Sosnica K., Zus F., Balidakis K., (2019): *Troposphere delay modeling with horizontal gradients for satellite laser ranging*, Journal of Geodesy, Vol. 93, No 10, Berlin-Heidelberg, Germany 2019, pp. 1853–1866. doi: 10.1007/s00190-019-01287-1
- Dykowski P., Kane P., Krynski J., Fitzpatrick K., Bell G., Aiken M., (2019a): *Towards the establishment of the Absolute Gravity Network Ireland*, Symposium of the IAG Subcommission for Europe (EUREF) held in Tallinn, Estonia, 22–24 May 2019 <http://www.euref.eu/symposia/2019Tallinn/03-03-Dykowski.pdf>
- Dykowski P., Krynski J., Sekowski M., (2019b): *A 3-year long AG/SG gravity time series at Borowa Gora Geodetic Geodetic-Geophysical Observatory*, 27 IUGG General Assembly 2019, Montreal, Canada, 08–18 July 2019.
- Dykowski P., Krynski J., Sekowski M., Kane P., Fitzpatrick K., Healy R., Byrne M., Bell G., Aiken M., (2019c): *Establishment of the Absolute Gravity Network Ireland – first results*, 5th IAG Symposium on Terrestrial Gravimetry: Static and Mobile Measurements TG-SMM, 1–4 October 2019, St. Petersburg, Russia.
- Dykowski P., Sekowski M., Krynski J., Olszewska D., Araszkiwicz A., Kaplon J., Borkowski A., Ilieva M., Mutke G., Kotyrba A., Baranski A., (2019d): *Gravity, GNSS, InSAR combination for monitoring deformation related to industrial activity on Multidisciplinary Upper Silesian Episode within the EPOS-PL project*, 5th IAG Symposium on Terrestrial Gravimetry: Static and Mobile Measurements TG-SMM, 1–4 October 2019, St. Petersburg, Russia.
- Engfeldt A., Lidberg M., Sekowski M., Dykowski P., Krynski J., Ågren J., Olsson P.-A., Bryskhe H., Steffen H., Nielsen J.E., (2019): *RG 2000 – the new gravity reference frame of Sweden*, FIG Congress 2018, 6–11 May 2018, Istanbul, Turkey; Geophysica, 54(1), pp. 69–92.
- Falk R., Pálinkáš V., Wziontek H., Rülke A., Val'ko M., Ullrich Ch., Butta H., Kostelecký J., Bilker-Koivula M., Näränen J., Prato A., Mazzoleni F., Kirbaş C., Coşkun I., Van Camp M., Casrelein S., Bernard J.D., Lothhammer A., Schilling M., Timmen L., Iacovone D., Nettis G., Greco F., Messina A.A., Reudink R., Petrini M., Dykowski P., Sekowski M., Janák J., Papčo J., Engfeldt A., Steffen H., (2020): *Final report of EURAMET.M.G-K3 regional comparison of absolute gravimeters*, Metrologia, Vol. 57, No 1A, doi: 10.1088/0026-1394/57/1A/07019
- Fenoglio L., Dinardo S., Uebbing B., Buchhaupt C., Gaertner M., Staneva J., Becker M., Klos A., Kusche J., (2020): *Advances in NE-Atlantic coastal sea level change monitoring by Delay Doppler altimetry*, Advances in Space Research. doi: 10.1016/j.asr.2020.10.041
- Godah W., Gedamu A.A., Bedada T.B., (2018): *On the contribution of dedicated gravity satellite missions to the modelling of the Earth gravity field – A case study of Ethiopia and Uganda in the East Africa*, Geoinformation Issues 10(1), pp. 5–15.
- Godah W., (2019): *IGiK-TVGMF: A MATLAB package for computing and analysing temporal variations of gravity/mass functionals from GRACE satellite based global geopotential models*, Computers & Geosciences, Vol. 123, pp. 47–58. <https://doi.org/10.1016/j.cageo.2018.11.008>
- Godah W., Gedamu A.A., Bedada T.B., (2019a): *On the contribution of dedicated gravity satellite mission to the modelling of the Earth gravity field over East Africa*, 27th IUGG General Assembly, Montréal, Canada, 8–18 July, 2019.
- Godah W., Szelachowska M., Ray J.D., Krynski J., (2019b): *A model of temporal mass variations within the Earth system developed using GRACE and GNSS data*, 27th IUGG General Assembly, Montréal, Canada, 8 – 18 July, 2019.
- Godah W., Szelachowska M., Ray J.D., Krynski J., (2019c): *On the determination of vertical displacements using GRACE and GNSS data – A case study of Poland*, ESA Living Planet Symposium, 13–17 May 2019, Milan, Italy.
- Godah W., Szelachowska M., Ray J.D., Krynski J., (2019d): *Comparison of vertical displacements obtained using GRACE data and GNSS data over Poland*, 20th Workshop on Recent Geodynamics of Central Europe and the 2nd Symposium of the Committee on Geodesy Polish Academy of Sciences, 24–26 October, Jakuszyce, Poland.
- Godah W., Szelachowska M., Ray J.D., Krynski J., (2019e): *On the recovery of temporal variations of geoid heights determined with the use of GGMs based on SST-hl data from non-dedicated gravity satellite missions*, Bulletin of Geodetic Sciences, 25(3): e2019017. doi: 10.1590/s1982-21702019000300017.
- Godah W., Szelachowska M., Ray D.D., Krynski J., (2020): *Comparison of vertical deformations of the Earth's surface obtained using GRACE-based GGMs and GNSS data – a case study of South-Eastern Poland*, Acta Geodyn. Geomater., Vol. 17, No 2(198), pp. 169–176. doi: 10.13168/AGG.2020.0012
- Godah W., Ray J.D., Szelachowska M., Krynski J., (2020a): *The Use of National CORS Networks for Determining Temporal Mass Variations within the Earth's System and for Improving GRACE/GRACE-FO Solutions*, Remote Sensing 12(20):3359. <https://doi.org/10.3390/rs12203359>
- Godah W., Szelachowska M., Krynski J., Ray J.D., (2020b): *Assessment of Temporal Variations of Orthometric/Normal Heights Induced by Hydrological Mass Variations over Large River Basins Using GRACE Mission Data*, Remote Sensing 12(18):3070. <https://doi.org/10.3390/rs12183070>
- Hadás T., Kazmierski K., Sosnica K., (2019): *Performance of Galileo-only dual-frequency absolute positioning using the fully serviceable Galileo constellation*, GPS Solutions, Vol. 23, No 108, Berlin-Heidelberg 2019, pp. 1–12. doi: 10.1007/s10291-019-0900-9
- Jagoda M., Rutkowska M., Lejba P., Katzer J., Obuchowski R., Šlikas D., (2020): *Satellite Laser Ranging for Retrieval of the Local Values of the Love h_2 and Shida l_2 Numbers for the Australian ILRS Stations*, Sensors 2020, 20(23): 6851, doi: 10.3390/s20236851.
- Jarmolowski W., Ren X., Wielgosz P., Krypiak-Gregorczyk A., (2018): *Assessment of Ionosphere TEC Determination From Dual-Frequency Altimetry Missions With Reference to Local and Global GNSS-TEC Models in Coastal*

- Regions, 25 Years of Progress in Radar Altimetry*, Symposium, Ponta Delgada, Portugal 24–29 September 2018.
- Jarmolowski W., (2019): *On the relations between signal spectral range and noise variance in least squares collocation and simple kriging: example of gravity reduced by EGM2008 signal*, *Bollettino di Geofisica Teorica et Applicata* 60(3): 457–474.
- Jarmolowski W., Ren X., Wielgosz P., Krypiak-Gregorczyk A., (2019a): *On the advantage of stochastic methods in the modeling of ionospheric total electron content: Southeast Asia case study*, *Measurement Science and Technology* 30 (4): 44008, <https://dx.doi.org/10.1088/1361-6501/ab0268>
- Jarmolowski W., Wielgosz P., Krypiak-Gregorczyk A., Ren X., (2019b): *Comparison of stochastic methods in interpolation and extrapolation of sparse GNSS TEC observations*, EGU General Assembly 2019, Vienna, Austria, 7–12 April 2019.
- Jarmolowski W., Wielgosz P., Krypiak-Gregorczyk A., Milanowska B., (2020): *Analysis of Swarm Electric Field Data in View of Tsunami Events and related Earthquakes*, EGU General Assembly 2020
- Jarmolowski W., Belehaki A., Hernández Pajares M., Goss A., Schmidt M.G., Wielgosz P., Yang H., Krypiak-Gregorczyk A., Tsagouri I., Paouris E., Monte-Moreno E., García-Rigo A., Erdogan E. Graffigna V., Milanowska B., Haagmans R., (2021): *Consolidation of Swarm electron density field observations with other LEO satellite data, ground GNSS and ionosonde observations in view of seismic ionospheric disturbances detection and prompt detection of tsunamis: an extensive case study of 2015 Chile-Illapel*. (under submission)
- Kaczmarek A., (2019): *Influence of Geophysical Signals on Coordinate Variations GNSS Permanent Stations in Central Europe*, Artificial Satellites, *Journal of Planetary Geodesy*, Vol. 54, No 3, Warsaw, Poland, pp. 57–71, doi: 10.2478/arsa-2019-0006.
- Karkowska K., Wilde-Piorko M., (2019): *How can gravimeters improve recordings of earthquakes?* Geophysical Research Abstract, Vol. 21, EGU2019-427, EGU General Assembly 2019, 7–12 April, Vienna, Austria, <https://meetingorganizer.copernicus.org/EGU2019/EGU2019-427.pdf>
- Karkowska K., Wilde-Piorko M., (2020): *Determination of the Earth's Structure Based on Long-Period Surface Wave Recordings of Tidal Gravimeters*, AGU Fall Meeting 2020, 1-17 December, G016-04
- Katsigianni G., Loyer S., Perosanz F., Mercier F., Zajdel R., Sosnica K., (2019): *Improving Galileo orbit determination using zero-difference ambiguity fixing in a Multi-GNSS processing*, *Advances in Space Research*, Vol. 63, No 9, 2019, pp. 2952–2963. doi: 10.1016/j.asr.2018.08.03
- Kaźmierski K., Zajdel R., Sosnica K., (2020): *Evolution of orbit and clock quality for real-time multi-GNSS solutions*, *GPS Solutions*, Vol. 24, No 111, pp. 1–12 doi: 10.1007/s10291-020-01026-6
- Kenyeres A., Bellet J.G., Bruyninx C., Caporali A., De Doncker F., Droszak B., Duret A., Franke P., Georgiev I., Bingley R., Huisman L., Jivall L., Khoda O., Kollo K., Kurt A.I., Lahtinen S., Legrand J., Magyar B., Mesmaker D., Morozova K., Nagl J., Ozdemir S., Papanikolaou X., Parseulinas E., Stangl G., Tangen O.B., Valdes M., Ryczywolski M., Zurutuza J., Weber M., (2019): *Regional integration of long-term national dense GNSS network solutions*, *GPS Solutions*, (2019) 23:122, <https://doi.org/10.1007/s10291-019-0902-7>
- Kiliszek D., Kroszczyński K., (2020): *Performance of the Precise Point Positioning method along with the development of GPS, GLONASS and Galileo systems*, *Measurement* 2020, 164, 108009. doi: 10.1016/j.measurement.2020.108009
- Klos A., Kusche J., Fenoglio-Marc L., Bos M.S., Bogusz J., (2019): *Introducing a vertical land motion model for improving estimates of sea level rates derived from tide gauge records affected by earthquakes*, *GPS Solutions*, 23:102, doi:10.1007/s10291-019-0896-1
- Klos A., Karegar M., Kusche J., Springer A., (2020): *Quantifying Noise in Daily GPS Height Time Series: Harmonic Function Versus GRACE Assimilating Modeling Approaches*, *IEEE Geoscience and Remote Sensing Letters*, doi:10.1109/LGRS.2020.2983045
- Konacki M., Malacz A., Chmicz A., Lejba P., Sybilski P., Pawlaszek R., Kozłowski S., Suchodolski T., Kozłowski K., Sybiliska A., Rogowska B., Pazderski D., Zolnowski M., Shearer A., Slowikowska A., Pilichowski M., Malawski M., Gedek M., (2019): *Optical, Laser and Processing Capabilities of the New Polish Space Situational Awareness Centre*, Advanced Maui Optical and Space Surveillance Technologies Conference (AMOS), 17–20 September, <https://amostech.com/2019-technical-papers/>
- Kotyrbra A., Kortas Ł., (2020): *Co-seismic signals of mining tremors in continuous recordings of gravity by gPhoneX tidal gravimeters*, *International Journal of Rock Mechanics and Mining Sciences* 129:10428, doi: 10.1016/j.ijrmms.2020.104288
- Kowalczyk K., (2019): *Changes In Mean Sea Level On The Polish Coast Of The Baltic Sea Based On Tide Gauge Data From The Years 1811-2015*, *Acta Geodynamica et Geomaterialia*, 16(2), 195–210.
- Kowalczyk K., Pajak K., Naumowicz B., (2019): *Modern Vertical Crustal Movements Of The Southern Baltic Coast From Tide Gauge, Satellite Altimetry And GNSS Observations*, *Acta Geodynamica et Geomaterialia*, 16(3), 245–253.
- Krynski J., Rogowski J.B., Liwosz T., (2019a): *Research on reference frames and reference networks in Poland in 2015-2018*, *Geodesy and Cartography*, Vol. 68, No 1, 2019, doi: 10.24425/gac.2019.126093
- Krynski J., Dykowski P., Olszak T., (2019b): *Research on gravity field modelling and gravimetry in Poland in 2015–2018*, *Geodesy and Cartography*, Vol. 68, No 1, 2019, doi: 10.24425/gac.2019.126094
- Krynski J., Olszewska D., Gorka-Kostrubiec B., Lizurek G., Jozwiak W., Werner T., Araszkievicz A., Czuba W., Sosnica K., Mutke G., Szepieniec T., (2019c): *EPOS PL Polish national infrastructure fulfilling European Plate Observing System goals*, 27 IUGG General Assembly 2019, Montreal, Canada, 08–18 July 2019.
- Krynski J., Rogowski J.B., (2019): *National Report of Poland to EUREF 2019*, Symposium of the IAG Subcommission for Europe (EUREF) held in Tallinn, Estonia, 22–24 May 2019, <http://www.euref.eu/symposia/2019Tallinn/05-19-p-Poland.pdf>
- Krypiak-Gregorczyk A., Wielgosz P., Jarmolowski W., Erdogan E., Goss A., Schmidt M., (2019): *Comparison of spatio-temporal ionosphere profiles obtained from GNSS and ionosonde data during severe ionospheric storm of 8th September 2017*, EGU General Assembly 2019, 7–12 April 2019, Vienna, Austria.
- Krzan G., Stepniak K., (2019a): *Impact of individual antenna phase center models on GNSS tropospheric estimates*, *Scientific and Fundamental Aspects of GNSS*, 4–6 Sept. 2019, Zurich, Switzerland.
- Krzan G., Stepniak K. (2019b): *Individual calibration antenna PCC models: differences and their impact on tropospheric estimates*, EPN Analysis Center Workshop, Warsaw, Poland, 16–17 October.

- Krzan G., Dawidowicz K., Wielgosz P., (2020): *Antenna phase center correction differences from robot and chamber calibrations: the case study LEIAR25*, GPS Solutions 24, 44.
- Kuczynska-Siehn J., Piretzidis D., Sideris M., Olszak T., Szabo V., (2019): *Monitoring of extreme land hydrology events in central Poland using GRACE, land surface models and absolute gravity data*, Journal of Applied Geodesy, Vol. 13, No 3, pp. 1–15, doi:10.1515/jag-2019-0003.
- Kudlacik I., Kaplon J., Bosy J., Lizurek G., (2019): *Seismic phenomena in the light of high-rate GPS Precise Point Positioning results*, Acta Geodyn. Geomater, 16, 99–112.
- Lejba P., Suchodolski T., Michalek P., (2020): *Laser Ranging to Space Debris in Poland: Tracking and Orbit Determination*, Proceeding of The Advanced Maui Optical and Space Surveillance Technologies Conference (AMOS), 15–18 September 2020, <https://amostech.com/2020-technical-papers/>
- Lenczuk A., Leszczuk G., Klos A., Kosek W., Bogusz J., (2020): *Study on the inter-annual hydrology-induced deformations in Europe using GRACE and hydrological models*, Journal of Applied Geodesy, Vol. 14, Issue 4, pp. 393–403, doi:10.1515/jag-2020-0017
- Liwosz T., (2019): *The report of WUT EPN Analysis Centre*, EPN Analysis Center Workshop, Warsaw, Poland, 16–17 October.
- Liwosz T., Araszkiewicz A., (2019a): *Report of the EPN Analysis Coordinator Report. Inclusion of Galileo observations in EPN coordinate products*, EUREF Symposium, Tallinn, Estonia, 22–24 May.
- Liwosz T., Araszkiewicz A., (2019b): *EPN Analysis Centres Coordinator Report*, EPN Analysis Center Workshop, Warsaw, Poland, 16–17 October 2019.
- Liwosz T., Pacione R., Brockmann E., (2019): *Usage of Galileo in EUREF Permanent Network Data and Products*, 7th International Colloquium on Scientific and Fundamental Aspects of GNSS, 4–6 September 2019, Zurich.
- Liu Z., (2011): *A new automated cycle slip detection and repair method for a single dual-frequency GPS receiver*, J Geod 85(3): 171–183. doi:10.1007/s00190-010-0426-y
- Lyszkowicz A., Bernatowicz A., (2018): *Absolute sea level changes at the tide gauge station in Wladyslawowo using different time series software package*, Geodesy, Cartography and Aerial Photography (ISTCGCAP), Vol. 88, No 88, pp. 13–23, <https://doi.org/10.23939/istcgcap.2018.02.013>
- Lyszkowicz A., Bernatowicz A., (2019): *Geocentric Baltic Sea level changes along the southern coastline*, Advance in Space Research, 64(2019) 1807–1815, <https://doi.org/10.1016/j.asr.2019.07.040>
- Lyszkowicz A., (2019): *Realization of the International Height Reference System – State of Art.*, Modern achievements of geodetic science and industry, Lviv Polytechnic National University, Issue I (37), pp. 51–60.
- Marjanska D., Olszak T., Pietka D., (2019): *Validation of European Gravimetric Geoid models in context of realization of EVRS system in Poland*, Geodesy and Cartography, Vol. 68, No 2, pp. 329–347, doi: 10.24425/gac.2019.128461
- Mota G.V., Song S., Stepniak K., (2019): *Assessment of Integrated Water Vapor Estimates from the iGMAS and the Brazilian Network GNSS Ground-Based Receivers in Rio de Janeiro*, Remote Sens. 2019, 11, 2652, doi: 10.3390/rs11222652
- Mutke G., Kotyrba A., Lurka A., Olszewska D., Dykowski P., Borkowski A., Araszkiewicz A., Baranski A., (2019): *Upper Silesian Geophysical Observation System A unit of the EPOS project*, Journal of Sustainable Mining, Vol. 18, Issue 4, November 2019, pp. 198–207, <https://doi.org/10.1016/j.jsm.2019.07.005>
- Nastula J., Winska M., Sliwinska J., Salstein D., (2019): *Hydrological signals in polar motion excitation – Evidence after fifteen years of the GRACE mission*, Journal of Geodynamics, 124(2018), pp. 119–132. <https://doi.org/10.1016/j.jog.2019.01.014>
- Nastula J., Sliwinska J., (2020): *Prograde and Retrograde Terms of Gravimetric Polar Motion Excitation Estimates from the GRACE Monthly Gravity Field Models*, Remote Sensing, 12(1), 138, 1–29. <https://doi.org/10.3390/rs12010138>
- Nowel K., Cellmer S., Fischer A., (2020): *Validation of GNSS baseline observation models using information criteria*, Survey Review, published online: 18 Jul 2020, doi: 10.1080/00396265.2020.1790168
- Nykiel G., Figurski M., Baldysz Z., (2019a): *Analysis of GNSS sensed precipitable water vapour and tropospheric gradients during the derecho event in Poland of 11th August 2017*, Journal of Atmospheric and Solar-Terrestrial Physics, 193, doi: 10.1016/j.jastp.2019.105082
- Nykiel G., Zanimonskiy Y., Koloskov A., Figurski M., (2019b): *The possibility of estimating the height of the ionospheric inhomogeneities based on TEC variations maps obtained from dense GPS network*, Advances in Space Research, 64(10), pp. 2002–2011, doi: 10.1016/j.asr.2019.06.008
- Otsubo T., Müller H., Pavlis E.C., Torrence M.H., Thaller D., Glotov V.D., Wang X., Sosnica K., Meyer U, Wilkinson M.J. (2019): *Rapid response quality control service for the laser ranging tracking network*, Journal of Geodesy, Vol. 93, No 11, pp. 2335–2344. doi: 10.1007/s00190-018-1197-0
- Öztürk E.Z., Godah W., Abbak R.A., (2020): *Estimation of Physical Height Changes from GRACE Satellite Mission Data over Turkey*, Acta Geodaetica et Geophysica 55(2): 301–317. <https://doi.org/10.1007/s40328-020-00294-5>
- Pajak K., Kowalczyk K. (2019): *A comparison of seasonal variations of sea level in the southern Baltic Sea from altimetry and tide gauge data*, Advances in Space Research, 63(5), 1768–1780.
- Paziewski J., Sieradzki R., Baryla R., (2019a): *Signal characterization and assessment of code GNSS positioning with low-power consumption smartphones*, GPS Solutions, 23:98, <https://doi.org/10.1007/s10291-019-0892-5>
- Paziewski J., Sieradzki R., Baryla R., (2019b): *Detection of Structural Vibration with High-Rate Precise Point Positioning: Case Study Results Based on 100 Hz Multi-GNSS Observables and Shake-Table Simulation*, Sensors 2019, 19(22), 4832, <https://doi.org/10.3390/s19224832>
- Paziewski J., Sieradzki R., (2020): *Enhanced wide-area multi-GNSS RTK and rapid static positioning in the presence of ionospheric disturbances*, Earth Planets and Space 72, 110 (2020). <https://doi.org/10.1186/s40623-020-01238-7>
- Paziewski J., Kurpinski G., Wielgosz P., Stolecki L., Sieradzki R., Seta M., Oszczak S., Castillo M., Martin-Porqueras F., (2020): *Towards Galileo + GPS seismology: Validation of high-rate GNSS-based system for seismic events characterisation*, Measurement, Vol. 166. <https://doi.org/10.1016/j.measurement.2020.108236>.
- Paziewski J., (2020): *Recent advances and perspectives for positioning and applications with smartphone GNSS observations*, Measurement Science and Technology 31(9) 091001. <https://doi.org/10.1088/1361-6501/ab8a7d>
- Pearlman M., Arnold D., Davis M., Barlier F., Biancale R., Vasiliev V., Ciufolini I., Paolozzi A., Pavlis E.C., Sosnica K., Bloßfeld M., (2019): *Laser geodetic satellites: a high-*

- accuracy scientific tool, *Journal of Geodesy*, Vol. 93, No 11, pp. 2181–2194. doi: 10.1007/s00190-019-01228-y
- Poniatowski M., Nykiel G., (2020): *Degradation of Kinematic PPP of GNSS Stations in Central Europe Caused by Medium-Scale Traveling Ionospheric Disturbances During the St. Patrick's Day 2015 Geomagnetic Storm*, *Remote Sensing*, 12, 3582, doi: 10.3390/rs12213582
- Ray J.D., Vijayan M.S.M., Godah W., (2021): *Seasonal Horizontal Deformations Obtained Using GPS and GRACE Data: Case Study of North-East India and Nepal Himalaya*, *Acta Geodaetica et Geophysica*. <https://doi.org/10.1007/s40328-020-00331-3>
- Rzepecka Z., Birylo M., (2020): *Groundwater Storage Changes Derived from GRACE and GLDAS on Smaller River Basins – A Case Study in Poland*, *Geosciences* 2020, 10(4), 124; <https://doi.org/10.3390/geosciences10040124>
- Schillak S., Lejba P., Michalek P., (2021): *Analysis of the Quality of SLR Station Coordinates Determined from Laser Ranging to the LARES Satellite*, *Sensors* 2021, 21(3), 737, doi: 10.3390/s21030737
- Schueller K., (2015): *Theoretical basis for Earth Tide analysis with the new ETERNA34-ANA-V4.0 program*, *Bull. Inf. Marées Terrestres*, 149, 12024–12061. <http://www.bim-icet.org>
- Sieradzki R., Paziewski J., (2018): *On the Feasibility of Interhemispheric Patch Detection Using Ground-Based GNSS Measurements*, *Remote Sensing*, Vol. 20(3), 2044, doi: 10.3390/rs10122044
- Sieradzki R., Paziewski J., (2019): *GNSS-based analysis of high latitude ionospheric response on a sequence of geomagnetic storms performed with ROTI and a new relative STEC indicator*, *Journal of Space Weather and Space Climate*, Vol. 9, doi: 10.1051/swsc/2019001
- Sliwinka J., Nastula J., (2019): *Determining and evaluating the hydrological signal in polar motion excitation from gravity field models obtained from kinematic orbits of LEO satellites*, *Remote Sensing*, 11(15), 1784, 1–19. <https://doi.org/10.3390/rs11151784>
- Sliwinka J., Winska M., Nastula J., (2019a): *Terrestrial water storage variations and their effect on polar motion*, *Acta Geophysica*, 67(1), pp. 17–39, <https://doi.org/10.1007/s11600-018-0227-x>
- Sliwinka J., Birylo M., Rzepecka Z., Nastula J., (2019b): *Analysis of groundwater and total water storage changes in Poland using GRACE observations, in-situ data, and various assimilation and climate models*, *Remote Sensing*, 11(24). <https://doi.org/10.3390/rs11242949>
- Sliwinka J., Nastula J., Dobsław H., Dill R., (2020a): *Evaluating Gravimetric Polar Motion Excitation Estimates from the RL06 GRACE Monthly-Mean Gravity Field Models*, *Remote Sensing*, 12(6), 930, 1–29. <https://doi.org/10.3390/rs12060930>
- Sliwinka J., Winska M., Nastula J. (2020b): *Preliminary estimation and validation of polar motion excitation from different types of the GRACE and GRACE FOLLOW-ON missions data*, *Remote Sensing*, 12(21), 1–28, doi: 10.3390/rs12213490
- Sosnica K., Bury G., Zajdel R., Strugarek D., Drozdowski M., Kazmierski K., (2019): *Estimating global geodetic parameters using SLR observations to Galileo, GLONASS, BeiDou, GPS, and QZSS*, *Earth Planets and Space*, Vol. 71, No 20, pp. 1–11. doi: 10.1186/s40623-019-1000-3
- Sosnica K., Zajdel R., Bury G., Bosy J., Moore M., Masoumi S., (2020): *Quality assessment of experimental IGS multi-GNSS combined orbits*, *GPS Solutions*, 24(2), 1–14.
- Specht C., Koc W., Chrostowski P., Szmaglinski J., (2019): *Accuracy Assessment of Mobile Satellite Measurements Relation to the Geometrical Layout of Rail Tracks*, *Metrol. Meas. Syst.*, 26(2), 309–321. doi: 10.24425/mms.2019.128359
- Specht, C., Wilk, A., Koc, W., Karwowski, K., Dabrowski, P., Specht, M., Grulowski S., Chrostowski P., Szmaglinski J., Czaplewski K., Skibicki J., Judek S., Licow, R., (2020): *Verification of GNSS measurements of the railway track using standard techniques for determining coordinates*, *Remote Sensing* 2020, 12(18), 2874, doi: 10.3390/rs12182874
- Strugarek D., Sosnica K., Arnold D., Jäggi A., Zajdel R., Bury G., Drozdowski M., (2019a): *Determination of Global Geodetic Parameters Using Satellite Laser Ranging Measurements to Sentinel-3 Satellites*, *Remote Sensing*, Vol. 11(19), No 2282, Basel, Switzerland 2019, pp. 1–21. doi: 10.3390/rs11192282
- Strugarek D., Sosnica K., Jäggi A., (2019b): *Characteristics of GOCE orbits based on Satellite Laser Ranging*. *Advances in Space Research*, Vol. 63, No 1, 2019, pp. 417–431. doi: 10.1016/j.asr.2018.08.033
- Suchodolski T., (2019): *CBK PAS Borowiec Second Satellite Tracking System*, ILRS Technical Workshop in Stuttgart, Germany, 21–25 October, https://cddis.nasa.gov/2019_Technical_Workshop/Program/index.html
- Szabó V., Marjanska D., (2020): *Accuracy analysis of gravity field changes from GRACE RL06 and RL05 data compared to in situ gravimetric measurements in the context of choosing optimal filtering type*, *Artificial Satellites, Journal of Planetary Geodesy*, 2020, Vol. 3, No 55, pp.1-19. doi: 10.2478/arsa-2020-0008
- Trojanowicz M., (2019): *Local disturbing potential model with the use of geophysical gravity data inversion - case study in the area of Poland*, *Acta Geodyn. Geomater.*, Vol. 16, No 3(195), pp 293–299, doi: 10.13168/AGG.2019.0025
- Trojanowicz M., Osada E., Karsznia K., (2020a): *Precise local quasigeoid modelling using GNSS/levelling height anomalies and gravity data*, *Survey Review* 52(730): 76–83. <https://doi.org/10.1080/00396265.2018.1525981>
- Trojanowicz M., Pospíšil L., Jamroz O., (2020b): *Use of the UNB_TOPODENS model for local modelling of chosen gravity field parameters in the western Carpathians*, *Acta Geodyn. Geomater.*, Vol. 17, No 1(197), 113–118, doi: 10.13168/AGG.2020.0008
- Trojanowicz M., Owczarek-Wesołowska M., Pospíšil L., Jamroz O., (2020c): *Determination of the Selected Gravity Field Functionals by the GGI Method: A Case Study of the Western Carpathians Area*, *Appl. Sci.* 2020, 10, 7892; doi: 10.3390/app10217892
- Vaclavovic P., Dousa J., (2016): *G-Nut/Anubis - open-source tool for multi-GNSS data monitoring*, In: *IAG Symposia Series*, Springer, Vol. 143, pp. 775–782, doi: 10.1007/1345_2015_157
- Werner T., Olszewska D., Gorka-Kostrubiec B., Lizurek G., Jozwiak W., Krynski J., Czuba W., Rohm W., Araszkievicz A., Mutke G., Sterzel M., Szepieniec T., Wojcik D., (2019): *EPOS PL – Polish national contribution towards EPOS infrastructure*, *Geophysical Research Abstracts*, Vol. 21, EGU2019-13968, EGU General Assembly 2019, 7–12 April, Vienna, Austria.
- Wielgosz P., Milanowska B., Krypiak-Gregorczyk A., (2019): *Validation of IGS IAAC maps during different solar activity levels: case studies for years 2014 and 2018*, 2nd International Workshop on GNSS Ionosphere (IWGI2019), DLR, 23–25 September 2019, Neustrelitz, Germany.
- Wilde-Piorko M., Karkowska K., (2019): *Improving the Determination of Earth's Mantle Structure by Continuous Gravimetric Records*, 27th IUGG 2019 General Assembly,

- Montreal, Canada, 8–18 July 2019, Abstract number: IUGG19-1337.
- Wilde-Piorko M., Karkowska K., (2020): *Determination of Phase-Velocity Dispersion Curves of Rayleigh Surface Waves from Tidal Gravimetric Recordings of Earthquakes*, AGU Fall Meeting 2020, 1–17 December, S062-0014, doi: 10.1002/essoar.10506023.1
- Wilde-Piorko M., Dykowski P., Karkowska K., Olszak T., Polkowski M., Sekowski M. (2019): *Determination and Verification of Relative Gravimeters' Transfer Function*, 27 IUGG General Assembly 2019, Montreal, Canada, 08–18 July 2019.
- Wilk A., Specht C., Koc W., Karwowski K., Skibicki J., Szmaglinski J., Chrostowski P., Dabrowski P., Specht M., Zienkiewicz M., Judek S., Skora M., Grulkowski S., (2020a): *Evaluation of the Possibility of Identifying a Complex Polygonal Tram Track Layout Using Multiple Satellite Measurements*, Sensors 2020, 20(16), 4408, doi: 10.3390/s20164408
- Wilk A., Koc W., Specht C., Judek S., Karwowski K., Chrostowski P., Czaplewski K., Dabrowski P., Grulkowski S., Licow R., Skibicki J., Specht M., Szmaglinski J., (2020b). *Digital Filtering of Railway Track Coordinates in Mobile Multi-Receiver GNSS Measurements*, Sensors 2020, 20(18), 5018, doi: 10.3390/s20185018
- Wilk A., Koc W., Specht C., Skibicki J., Judek S., Karwowski K., Chrostowski P., Szmaglinski J., Dabrowski P., Czaplewski K., Specht M., Licow R., Grulkowski S., (2021), *Innovative mobile method to determine railway track axis position in global coordinate system using position measurements performed with GNSS and fixed base of the measuring vehicle*, Measurement 2021, 175, 109016, doi: 10.1016/j.measurement.2021.109016
- Zajdel R., Sosnica K., Dach R., Bury G., Prange L., Jäggi A., (2019a): *Network effects and handling of the geocenter motion in multi-GNSS processing*, Journal of Geophysical Research-Solid Earth, Vol. 124, No 6, Washington, DC, USA 2019, pp. 5970-5989. doi: 10.1029/2019JB017443
- Zajdel R., Sosnica K., Drozdowski M., Bury G., Strugarek D., (2019b): *Impact of network constraining on the terrestrial reference frame realization based on SLR observations to LAGEOS*, Journal of Geodesy, Vol. 93, No 11, pp. 2293–2313. doi: 10.1007/s00190-019-01307-0
- Zajdel R., Sosnica K., Bury G., Dach R., Prange L., (2020): *System-specific systematic errors in Earth rotation parameters derived from GPS, GLONASS, and Galileo*, GPS Solutions, Vol. 24, No 74, pp. 1–14. doi: 10.1007/s10291-020-00989-w
- Zajdel R., Sosnica K., Bury G., Dach R., Prange L., Kazmierski K., (2021a): *Sub-daily polar motion from GPS, GLONASS, and Galileo*, Journal of Geodesy, Vol. 95, No 3. <https://doi.org/10.1007/s00190-020-01453-w>
- Zajdel R., Sosnica K., Bury G., (2021b): *Geocenter coordinates derived from multi-GNSS: a look into the role of solar radiation pressure modelling*, GPS Solutions, Vol. 25, No 1. doi: <https://doi.org/10.1007/s10291-020-01037-3>